

Linear- T Resistivity from Spatially Random Vector Coupling

Xian-Hui Ge,^a Sang-Jin Sin,^b Yi-Li Wang^b

^a*Department of Physics, Shanghai University,
99 Shangda Rd., Shanghai, 200444, P.R. China*

^b*Department of Physics, Hanyang University,
222 Wangsimni-ro, Seoul, 04763, Korea*

E-mail: gexh@shu.edu.cn, sjsin@hanyang.ac.kr, wangyili@hanyang.ac.kr

ABSTRACT: Recently, Patel et.al introduced a higher dimensional version of the SYK model with random coupling in Yukawa interaction to find the linear- T resistivity. We test the universality of the mechanism by replacing the scalar with vector field in various dimensions. We find that it works for vector as well as scalar interaction, although the details are very different. However, this mechanism for the linear- T resistivity works only in $(2 + 1)$ dimension not in higher dimension independent of the interaction type. Based on these results, we explore the role of spatial random disorder and find a simple understanding how such random scattering converts the Fermi liquid to the strange metal by changing the behavior of the self-energies of involved boson and fermion.

Contents

1	Introduction	1
2	The Critical Fermi Surface Randomly Coupled to a $U(1)$ Gauge Field	2
2.1	The Model and Saddle Point Equation	2
2.2	Conductivity	6
3	Breakdown of Linear-T Resistivity in Higher Dimensions	12
3.1	Three dimensional Fermi surface coupled with gauge field	13
3.2	Random Yukawa coupling model in 3+1 dimension	16
4	The Emergence of Linearity: Fermi Liquid vs Strange Metal	19
5	Conclusion and Outlooks	24
A	A brief Summary of a few Models	25

1 Introduction

The strange-metallicity and its understanding is considered as one of the most important topics in modern physics [1–7], because it ubiquitous appears in metallic phase the strongly interacting systems as well as the normal phase of the high-temperature superconductors. While its property is simple and universal characterised by linear- T resistivity, its understanding has been scarce.

The strange metal violates various features of the Landau’s Fermi liquid as observed in several systems such as cuprate superconductors and heavy-fermion materials [5, 7–9]. It is often accompanied by a logarithmic specific heat proportional to $T \ln(1/T)$ [6], which indicates the existence of a quantum criticality [10–13]. Moreover, the resistivity coefficient A in $\rho = \rho_0 + AT$ is found to be closely related to the critical temperature T_c such that $T_c \sim A^\square$ [7]. A also is known to be correlated with superfluid density [1, 7]. All these observations were waiting a theory of strange metal, which is expected to be the key to comprehend the high-temperature superconductivity. Despite the tremendous efforts of the decades, the strange metal remains mysterious.

Very recently, however, inspired by the Sachdev-Ye-Kitaev (SYK) model [14–16] the authors of [17] attacked the problem using the spatial random couplings and achieved the strange-metal behaviour by randomising a Yukawa interaction $g\phi\psi^\dagger\psi$ between a Fermi surface (FS) and critically fluctuating scalar bosons [3, 17–19], where ψ and ϕ represents the electron and scalar field respectively. The interaction reads $g_{ijk}(\mathbf{r})\psi_i^\dagger\psi_j\phi_k$ with position dependent coupling constant, and $g_{ijk}(\mathbf{r})$ has zero mean and non-vanishing correlation

$\langle g_{ijk}^*(\mathbf{r})g_{i'j'k'}(\mathbf{r}') \rangle = g^2\delta(\mathbf{r} - \mathbf{r}')\delta_{ii'jj'kk'}$. This model bridged the chasm between the observations and the theoretical interpretation of strange metal for the first time.

It is of great interest to see how universal this mechanism is as a theory of strange metal. For this end, we extend the random Yukawa model in [17] to the vector coupling analogous to the QED to calculate its optical conductivity. In other words, we will consider an FS coupled to a $U(1)$ gauge field, where the coupling constant is spatially randomised. It will be shown that the linear- T resistivity still remains in this model although the details are different.

The rest of this article is organised as follows. In section 2, we build a system with a spatially random coupling between an FS and a $U(1)$ gauge field. After the corresponding ‘ G - Σ ’ action is constructed following [17–24], we will show that such a system exhibits strange-metallicity in $(2 + 1)$ dimensions. In section 3, we generalize our model as well as that of Patel et.al to $(3 + 1)$ -dimensional space-time, and show that linear- T resistivity is no more there. In section 4, we explore the role of spatial random disorder and find a simple mechanism how such random scattering converts the Fermi liquid to the strange metal by changing the propagators of bosons and fermions. Conclusion and outlooks comes in section 5.

2 The Critical Fermi Surface Randomly Coupled to a $U(1)$ Gauge Field

2.1 The Model and Saddle Point Equation

Let us start with a two-dimensional spinless electron gas coupled to a $U(1)$ gauge field. The action of such preliminary model reads in Euclidean time τ , [16, 25–28] :

$$S_{pre} = \int d\tau d^2\mathbf{r} \left[\psi^\dagger(\mathbf{r}, \tau) \left(\partial_\tau - \frac{\nabla^2}{2m} - \mu \right) \psi(\mathbf{r}) + v(\mathbf{r})\psi^\dagger(\mathbf{r}, \tau)\psi(\mathbf{r}, \tau) + \frac{1}{2}((\nabla \times \mathbf{A})^2 - \dot{A}^2) - e\psi^\dagger(\mathbf{r}, \tau) \left(i\phi - \frac{i}{m}\mathbf{A}\nabla \right) \psi(\mathbf{r}, \tau) + \frac{e^2}{2m}\mathbf{A}\mathbf{A}\psi^\dagger(\mathbf{r}, \tau)\psi(\mathbf{r}, \tau) \right], \quad (2.1)$$

where $\phi = a_0$ is the scalar potential and $\mathbf{A} = (A_x, A_y)$ is the vector potential. A spatial disorder is introduced by $v(\mathbf{r})$, known as a potential disorder featuring the scattering impurities [17, 18, 25, 29]. Here m and e respectively denote the bare mass and bare charge of an electron. Containing no topological term, this is not a suitable theory for studying the half-filled Landau level. However, as the simplest model one can have, (2.1) offers a reasonable starting point for future generalisation to more complicated and physically interesting systems. In action (2.1), the time derivative is included to make the action as general as possible, though this part will become subdominant during the computation [16].

We follow the strategy suggested in [17–19], and introduce spatial randomness to the interaction between the FS and the $U(1)$ gauge field. In order to trace the effects of random coupling, we replace e with K and e^2 by \tilde{K} and treat K and \tilde{K} as two independent parameters and randomise them separately. We take the result as our model. Then, our

action (2.1) can be written as

$$\begin{aligned}
S = \int d\tau d^2\mathbf{r} & \left[\sum_{ijl} \psi_i^\dagger(\mathbf{r}, \tau) \left(\partial_\tau - \frac{\nabla^2}{2m} - \mu \right) \psi_l(\mathbf{r}, \tau) + \frac{1}{\sqrt{N}} \sum_{ij} v_{ij}(\mathbf{r}) \psi_i^\dagger(\mathbf{r}, \tau) \psi_j(\mathbf{r}, \tau) \right. \\
& - \frac{1}{\sqrt{N}} \sum_{ij} K_{ij}(\mathbf{r}) \psi_i^\dagger(\mathbf{r}, \tau) \left(i\phi - \frac{i}{m} \mathbf{A} \cdot \nabla \right) \psi_j(\mathbf{r}, \tau) \\
& \left. + \frac{1}{\sqrt{N}} \sum_{ijab} \frac{\tilde{K}_{ij}(\mathbf{r})}{2m} \mathbf{A} \cdot \mathbf{A} \psi_i^\dagger \psi_j + \frac{1}{2} ((\nabla \times \mathbf{A})^2 - \dot{A}^2) \right]. \tag{2.2}
\end{aligned}$$

Following [17–19], we assume that v_{ij} , K_{ij} , and \tilde{K}_{ij} obey the Gaussian distribution with zero mean and satisfy

$$\langle v_{ij}^*(\mathbf{r}) v_{i'j'}(\mathbf{r}') \rangle = v^2 \delta(\mathbf{r} - \mathbf{r}') \delta_{ii'} \delta_{jj'}, \tag{2.3}$$

$$\langle K_{ij}^*(\mathbf{r}) K_{i'j'}(\mathbf{r}') \rangle = K^2 \delta(\mathbf{r} - \mathbf{r}') \delta_{ii'} \delta_{jj'}, \tag{2.4}$$

$$\langle \tilde{K}_{ij}^*(\mathbf{r}) \tilde{K}_{i'j'}(\mathbf{r}') \rangle = \tilde{K}^2 \delta(\mathbf{r} - \mathbf{r}') \delta_{ii'} \delta_{jj'}. \tag{2.5}$$

Unlike the random Yukawa coupling [30], our gauge field A^μ is not labeled by a flavour i .

There are two standard lore before moving on. First, the kinetic kernel of $U(1)$ gauge fields has no inverse in general [31], so gauge-fixing is necessary to get the propagator. It is convenient to choose a *Coulomb gauge* such that $\nabla \cdot \mathbf{A} = 0$ [16, 27–29, 31, 32], so the spatial part of the gauge field is transverse. Furthermore, for simplicity, the scalar potential ϕ is set to be $\phi = 0$ assuming that there is no external charge source. In any case, the gauge field A_μ has only one degree of freedom transverse to the spatial momenta \mathbf{q} , and this component is labeled by A_1 .

Next, we need a ‘ G - Σ ’ theory to study the large- N limit of the theory [17–24]. To write the action (2.2) in a standard form that describes an FS coupled to an emergent gauge field, we rescale $KA_\mu = a_\mu$ [26, 27, 33–37]. Let $\Sigma/\Pi^{\mu\nu}$ and $G/D^{\mu\nu}$ denotes the self-energy/polarisation and propagator of the fermion/gauge field. The optical conductivity can be directly read from the polarisation tensor of the gauge field through the Kubo formula. The key idea of G - Σ theory is to introduce a set of bilocal variables

$$G(x_1, x_2), \quad D^{\mu\nu}, \quad \Sigma(x_1, x_2), \quad \Pi^{\mu\nu},$$

and these will yield the propagators and self-energies at the saddle point where

$$\delta S / \delta G = \delta S / \delta \Sigma = \delta S / \delta D^{\mu\nu} = \delta S / \delta \Pi^{\mu\nu} = 0,$$

with $x = (\tau, \mathbf{r})$. The bi-local variables G and D are defined as follows,

$$G(x_1, x_2) \equiv -\frac{1}{N} \sum_i \langle \mathcal{T} \left(\psi_i(x_1) \psi_i^\dagger(x_2) \right) \rangle, \tag{2.6}$$

$$D^{\mu\nu}(x_1, x_2) \equiv \langle \mathcal{T} \left(a^\mu(x_1) a^\nu(x_2) \right) \rangle. \tag{2.7}$$

Together with these bi-local variables $G(x_1, x_2)$ and $D^{\mu\nu}(x_1, x_2)$, the 'self energies' $\Sigma, \Pi_{\mu\nu}$ are added as Lagrangian multipliers so that the G - Σ action reads

$$\begin{aligned}
S = \int d\tau d^2\mathbf{r} & \left[\sum_{ijl} \psi_i^\dagger(\mathbf{r}, \tau) \left(\partial_\tau - \frac{\nabla^2}{2m} - \mu \right) \psi_i(\mathbf{r}, \tau) + \frac{1}{\sqrt{N}} \sum_{ij} v_{ij}(\mathbf{r}) \psi_i^\dagger(\mathbf{r}, \tau) \psi_j(\mathbf{r}, \tau) \right. \\
& \left. + \frac{1}{2K^2} a^\mu (-\partial_\tau^2 + \mathbf{q}^2) a^\nu + \sum_{ij} \frac{1}{K\sqrt{N}} K_{ij} \psi_i^\dagger \frac{i}{m} \mathbf{a} \cdot \nabla \psi_j + \frac{1}{K^2\sqrt{N}} \sum_{ij} \frac{\tilde{K}_{ij}}{2m} \mathbf{a} \mathbf{a} \psi_i^\dagger \psi_j \right] \\
& - N \int d\tau d\tau' d^3\mathbf{r} \Sigma \left(G + \frac{1}{N} \sum_i \psi_i \psi_i^\dagger \right) + \frac{1}{2} \int d\tau d\tau' d^3\mathbf{r} \Pi^{\mu\nu} (D_{\mu\nu} - a_\mu a_\nu). \quad (2.8)
\end{aligned}$$

Performing disorder average via the replica trick [25] using the fact [25]

$$\int d(\psi, \psi^\dagger) e^{-(\psi^\dagger)^T M \psi} = \det(M),$$

for generic complex matrices M , one gets

$$\begin{aligned}
\frac{S}{N} = & -\ln \det((\partial_\tau + \varepsilon_k - \mu)\delta(x - x') + \Sigma) \\
& + \frac{1}{2} \ln \det\left(\frac{1}{K^2}(-\partial_\tau^2 + \mathbf{q}^2)\delta(x - x') - \Pi_{11}\right) \\
& + \text{Tr}\left(\frac{v^2}{2} G \cdot G\bar{\delta}\right) + \frac{1}{2m^2} \text{Tr}\left(\frac{(k_1 + k_2)^1(k_1 + k_2)^1}{4} G(k_1) D_{11} \cdot G(k_2)\bar{\delta}\right) \\
& + \text{Tr}\left(\frac{1}{8m^2} G D_{11} D^{11} \bar{\delta} G\right) - \text{Tr}(\Sigma \cdot G) + \frac{1}{2} \text{Tr}(\Pi^{11} D_{11}), \quad (2.9)
\end{aligned}$$

where \mathbf{k} is the momentum of fermions and $\bar{\delta}$ is the spatial delta function coming from the random average. Because $\phi = 0$ and $\nabla \cdot \mathbf{a} = 0$, only D_{11} and Π_{11} is non-trivial. Here $\varepsilon_{\mathbf{k}}$ is the fermion spectrum $\omega = \varepsilon_{\mathbf{k}} = \mathbf{k}^2/(2m)$ [29]. We use following short handed notation [18, 38],

$$\text{Tr}(f_1 \cdot f_2) \equiv f_1^T f_2 \equiv \int dx_1 dx_2 f_1(x_2, x_1) f_2(x_1, x_2), \quad (2.10)$$

where the transpose reads $f^T(x_1, x_2) \equiv f(x_2, x_1)$. Finally, starting from the action (2.9), one derives the saddle-point equation

$$\begin{aligned}
\frac{\delta S}{N} = & \text{Tr} \delta \Sigma \left((-\partial_\tau - \varepsilon_k + \mu - \Sigma)^{-1} - G \right) \\
& + \frac{1}{2} \text{Tr} \delta D^{11} \left(\Pi_{11} + \frac{1}{m^2} \frac{(k_1 + k_2)_1(k_1 + k_2)_1}{4} G \cdot G\bar{\delta} + \frac{1}{4m^2} G D_{\mu\nu} G\bar{\delta} \right) \\
& + \text{Tr} \delta G \left(-\Sigma + v^2 G\bar{\delta} + \frac{1}{m^2} \frac{(k_1 + k_2)^1(k_1 + k_2)^1}{4} D_{11} G\bar{\delta} + \frac{1}{4m^2} D_{\mu\nu} D^{\mu\nu} G\bar{\delta} \right) \\
& + \frac{1}{2} \text{Tr} \delta \Pi^{11} (D_{11} - K^2((-\partial_\tau^2 + \mathbf{q}^2) + K^2 \Pi^{11})^{-1}) \quad (2.11) \\
\equiv & \text{Tr} \left(\delta \Sigma (G_*[\Sigma] - G) + \delta G (\Sigma_*[G] - \Sigma) + \frac{1}{2} \delta \Pi_{11} (D^{11} - D_*^{11}[\Pi^{11}]) + \delta D_{11} (\Pi^{11} - \Pi_*^{11}[D_{11}]) \right),
\end{aligned}$$

where $k_\mu = (0, \mathbf{k})$. One then obtains the Dyson equations

$$G = G_* = (-\partial_\tau - \varepsilon_k + \mu - \Sigma)^{-1}, \quad (2.12)$$

$$\Sigma = \Sigma_* = v^2 G(\tau, \mathbf{r} = 0) \delta^3(\mathbf{r}) + \frac{(k_1 + k_2)_1 (k_1 + k_2)_1}{4m^2} D_{11} G \bar{\delta} + \frac{1}{4m^2} D_{11} D^{11} G \bar{\delta}, \quad (2.13)$$

$$D_{11} = D_{*11} = K^2 ((-\partial_\tau^2 + \mathbf{q}^2) - K^2 \Pi^{11})^{-1}, \quad (2.14)$$

$$\Pi_{11} = \Pi_{*11} = -\frac{(k_1 + k_2)_1 (k_1 + k_2)_1}{4m^2} G \bar{\delta} \cdot G - \frac{1}{4m^2} G D_{11} G \bar{\delta}, \quad (2.15)$$

which take similar forms with those found in [27], and they can be directly evaluated via Feynman diagrams. Considering low-frequency fermionic self-energies [17–19] up to one-loop corrections [27], the Feynman diagram corresponding to DDG term in eqn. (2.13)



$$, \quad (2.16)$$

where the dashed line represents the disorder average. This term can be neglected since it is quadratic in frequency. Here, the solid line and the wavy line represent the electron propagator and the gauge field propagator respectively ¹.

For the same reason, the terms GGD in eqn. (2.15), which corresponds to the following Feynman diagram



$$, \quad (2.17)$$

is also negligible. However, when we compute the conductivity later after coupling the system with an external electromagnetic field A_μ , this diagram is the key to linear resistivity, as will be shown later. In the presence of an external field, the polarisation (2.17) comes from $A_\mu a^\mu \psi^\dagger \psi$, which yields higher-order corrections in frequencies in [27], and this does not exist in [17]. In our model, this polarisation is not of higher order, so it will be computed as well.

Additionally, due to the fact $\langle \tilde{K}_{ij} \rangle = 0$, there is neither one-loop corrections to the fermionic self energy coming from



$$, \quad (2.18)$$

nor the gauge field polarisations coming from



$$, \quad (2.19)$$

¹Due to the spatial delta $\bar{\delta}$ in self-energies (2.13) and (2.15), the vertices of the propagators in these diagrams should be contracted. Here we use the ordinary Feynman diagram for clarity.

in our theory. This is notable difference from the system considered in [27].

2.2 Conductivity

In this work, the field a_μ plays a rôle similar to the scalar field in [26, 27, 33–37], so its polarisation (2.15) will be a straightforward measure of the optical conductivity. In principle, the conductivity shows the response of a system to the total electromagnetic field consisting of a_μ and an external electromagnetic field A_μ . Regardless of the origin of a_μ , the total electromagnetic field can be approximated by the external field A_μ [26].

Because of the spatial delta $\bar{\delta}$ in eqn.(2.13) and eqn.(2.15), the momentum dependence of the self-energies is lost, i.e. $\Sigma(i\omega_n, \mathbf{k}) = \Sigma(i\omega_n)$ and $\Pi_{ab}(i\Omega_m, \mathbf{q}) = \Pi_{ab}(i\Omega_m)$, with ω_n, Ω_m being the Matsubara frequencies. We begin with the evaluation of the electron self-energy Σ , letting $\xi_{\mathbf{k}} \equiv \varepsilon_{\mathbf{k}} - \mu$. The dominant part of electron self-energy comes from the potential disorder (like that in [17, 18]), which reads

$$\begin{aligned} \Sigma_v(i\omega_n) &= v^2 \int \frac{d^3\mathbf{k}'}{(2\pi)^3} G(i\omega_n, \mathbf{k}') \\ &= v^2 \int \mathcal{N} d\xi_{\mathbf{k}'} \frac{1}{i\omega_n - \xi_{\mathbf{k}'} - \Sigma(i\omega_n, \mathbf{k}')} \\ &= -i \frac{\Gamma}{2} \text{sgn}(\omega_n), \end{aligned} \tag{2.20}$$

where $\Gamma \equiv 2\pi v^2 \mathcal{N}$ is the disorder scattering rate, and $\mathcal{N} = m/(2\pi)$ is the Density of State (DoS) at the Fermi energy in two (spatial) dimensions. Here the integration over momentum $\int d\mathbf{k}$ can be replaced by the energy integral $\int d\xi_{\mathbf{k}}$ because the main contribution is from the electrons near the FS [29]. It can be verified later that the typical peak of electron propagator is wider than that of the gauge field, so we do not simplify the calculation via a Prange-Kadanoff reduction used in [18] on the saddle point.

Eqn.(2.13) implies that the computation of fermionic self-energies requires finding the bosonic propagator first. To this end, we need to find the bosonic self-energy (2.15). Due to the spatial delta, the vertices w and w' in usual bosonic contracts, and one obtains a graph with one vertices and two loops as follows,



The diagram illustrates the contraction of two vertices, w and w' , into a single vertex with two loops. On the left, two vertices are connected by two lines forming a loop. An arrow points to the right, where a single vertex is shown with two loops attached to it. The equation number (2.21) is located to the right of the diagram.

As a result, the bosonic self-energy reads

$$\begin{aligned}
& -K^2 \Pi_0^{11}(i\Omega_m) \\
&= \frac{K^2}{4m^2} \mathcal{N}^2 \int \frac{d\omega_n}{2\pi} \int d\xi_{\mathbf{k}} d\xi_{\mathbf{k}'} \frac{k_F^2}{i\frac{\Gamma}{2} \text{sgn}(\omega_n) - \xi_{\mathbf{k}}} \left(\frac{1}{i\frac{\Gamma}{2} \text{sgn}(\omega_n + \Omega_m) - \xi_{\mathbf{k}'}} - \frac{1}{i\frac{\Gamma}{2} \text{sgn}(\omega_n) - \xi_{\mathbf{k}'}} \right) \\
&= -\frac{i}{2} K^2 \frac{v_F^2}{4} \mathcal{N}^2 \delta^{\mu\nu} \int d\omega_n \int d\xi_{\mathbf{k}'} \text{sgn}(\omega_n) \left(\frac{1}{i\frac{\Gamma}{2} \text{sgn}(\omega_n + \Omega_m) - \xi_{\mathbf{k}'}} - \frac{1}{i\frac{\Gamma}{2} \text{sgn}(\omega_n) - \xi_{\mathbf{k}'}} \right) \\
&= -\frac{\pi}{2} K^2 \frac{v_F^2}{4} \mathcal{N}^2 \int d\omega_n \text{sgn}(\omega_n) (\text{sgn}(\omega_n + \Omega_m) - \text{sgn}(\omega_n)) \\
&= \pi \mathcal{N}^2 K^2 \frac{v_F^2}{4} |\Omega_m| \\
&\equiv c_0 |\Omega_m|, \tag{2.22}
\end{aligned}$$

with v_F the Fermi velocity. As we are interested in low temperatures, the Mastubara summation $T \sum_{\omega_n}$ is interchangeable with the integral $\int d\omega_n/(2\pi)$ [17–19, 25].

Now let's turn to the electron self-energy. The one-loop correction to electronic self-energy from eqn. (2.13) is graphically represented by


(2.23)

So there is also an contraction of vertex w and w' as illustrated below,


(2.24)

This self-energy can be written and gives

$$\begin{aligned}
\Sigma_K(i\omega_n) &= \frac{K^2}{4m^2} \int \frac{d\Omega_m}{2\pi} \int \frac{d^2\mathbf{q}}{(2\pi)^2} d\xi_{\mathbf{k}} \frac{k_F^2}{i\frac{\Gamma}{2} \text{sgn}(\omega_n + \Omega_m) - \xi_{\mathbf{k}}} \frac{1}{\mathbf{q}^2 + c_0 |\Omega_m|} \\
&= -iv_F^2 K^2 \frac{\mathcal{N}}{8} \int_{-\infty}^{+\infty} d\Omega_m \int_0^{\infty} \frac{|\mathbf{q}| d|\mathbf{q}|}{2\pi} \text{sgn}(\omega_n + \Omega_m) \frac{1}{|\mathbf{q}|^2 + c_0 |\Omega_m|} \\
&= -iK^2 \frac{v_F^2}{32\pi} \mathcal{N} \int d\Omega_m \text{sgn}(\omega_n + \Omega_m) \ln \left(\frac{\Lambda_q^2}{c_0 |\Omega_m|} \right) \\
&= -iK^2 v_F^2 \frac{\mathcal{N}}{16\pi} \omega_n \ln \left(\frac{e\Lambda_q^2}{c_0 |\omega_n|} \right), \tag{2.25}
\end{aligned}$$

where Λ_q is the UV cut-off on \mathbf{q} and e is the Euler's number (which should not be confused with the charge e). Therefore, we obtained a marginal Fermi liquid self-energy $\sim \omega \ln(1/\omega)$ [9, 17]. This self-energy will be translated to a specific heat $\sim T \ln(1/T)$, which is one of the features of strange metal. Let us emphasis again that there is no momentum conservation

imposed on the vertices, which can be seen from eqn.(2.25).

We are now ready to add an external field A_μ and find the current-current correlator (the polarization). The leading order polarization comes from square of the $A_\mu \psi^\dagger \nabla \psi$ coupling,



$$(2.26)$$

where the dotted wavy lines represent the external gauge field line. Due to the spatial delta, the polarisation and the bosonic self-energies are completely different. In order to distinguish these two quantities, let us denote the polarisation with $\tilde{\Pi}_{\mu\nu}$. The basic polarisation (2.26) is

$$\begin{aligned} \tilde{\Pi}_0^{11}(i\Omega_m) &= \frac{1}{2m^2} \mathcal{N} \int \frac{d\omega_n}{2\pi} \int d\xi_{\mathbf{k}} \frac{k_F^2}{i\omega_n + i\frac{\Gamma}{2} \text{sgn}(\omega_n) - \xi_{\mathbf{k}}} \\ &\times \left(\frac{1}{i(\omega_n + \Omega_m) + i\frac{\Gamma}{2} \text{sgn}(\omega_n + \Omega_m) - \xi_{\mathbf{k}}} - \frac{1}{i\omega_n + i\frac{\Gamma}{2} \text{sgn}(\omega_n) - \xi_{\mathbf{k}}} \right) \\ &= i\frac{v_F^2}{2} \mathcal{N} \frac{1}{2} \int d\omega_n \frac{\text{sgn}(\omega_n) - \text{sgn}(\omega_n + \Omega_m)}{i\frac{\Gamma}{2} \text{sgn}(\omega_n) - i\frac{\Gamma}{2} \text{sgn}(\omega_n + \Omega_m) - i\Omega_m} \\ &= \frac{v_F^2}{2} \mathcal{N} \frac{1}{\Gamma - \Omega_m} |\Omega_m| \equiv \frac{n_e}{m} \frac{1}{\Gamma - \Omega_m} |\Omega_m|, \end{aligned} \quad (2.27)$$

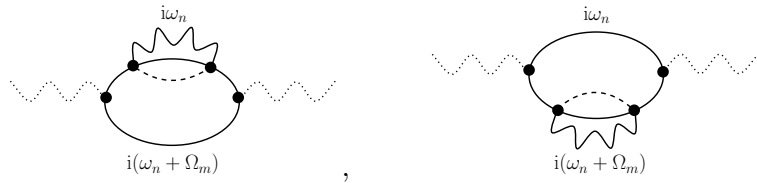
where n_e is the equilibrium density of electrons defined by $\mathcal{N}v_F^2/2 = n_e/m$. Notice that there is no sum over spins because the fermions in this model are spinless. The eqn.(2.27) describes the simplest contribution to the current-current correlator and will yields a Drude-like form after one applies the Kubo formula [18].

At low frequencies,

$$\tilde{\Pi}_0^{11}(i\Omega_m) = \frac{n_e}{m} \frac{1}{\Gamma} |\Omega_m| + \mathcal{O}(\Omega_m^2), \quad (2.28)$$

which is similar to the results in [17].

The Feynman diagrams representing the contribution of eqn.(2.25) to the polarizations are



$$(2.29)$$

The two diagrams bring the same contribution [17], which reads


$$\begin{aligned}
\tilde{\Pi}_{K(2)}^{11}(i\Omega_m) &= \tilde{\Pi}_{K(1)}^{11}(i\Omega_m) \\
&= \frac{1}{m^2} \mathcal{N} \int \frac{d\omega_n}{2\pi} \int d\xi_{\mathbf{k}} k^1 k^1 \left(\frac{1}{i\frac{\Gamma}{2} \text{sgn}(\omega_n) - \xi_{\mathbf{k}}} \right)^2 \frac{1}{i\frac{\Gamma}{2} \text{sgn}(\omega_n + \Omega_m) - \xi_{\mathbf{k}}} \Sigma_K(i\omega_n) \Big|_{\Omega_m=0}^{\Omega_m} \\
&= i \frac{K^2}{4} v_F^2 \mathcal{N} \int d\omega_n \frac{-\text{sgn}(\omega_n + \Omega_m) + \text{sgn}(\omega_n)}{(i\frac{\Gamma}{2} \text{sgn}(\omega_n + \Omega_m) - i\frac{\Gamma}{2} \text{sgn}(\omega_n))^2} \left[-i v_F^2 \omega_n \frac{\mathcal{N}}{16\pi} \ln \left(\frac{e\Lambda_q^2}{c_0 |\omega_n|} \right) \right] \\
&= -\frac{K^2}{128\pi} v_F^4 \frac{\mathcal{N}^2}{\Gamma^2} \Omega_m^2 \ln \left(\frac{e^3 \Lambda_q^4}{c_0^2 |\Omega_m|^2} \right). \tag{2.30}
\end{aligned}$$

In addition, there are vertex corrections coming from the Maki-Thompson diagrams (MT) diagrams,



$$, \tag{2.31}$$

and Aslamazov-Larkin (AL) diagrams



$$. \tag{2.32}$$

In [17], MT graphs and AL graphs vanish due to the spatial delta, which will be illustrated in section 4. In our case, though AL graphs are also zero for the same reason, MT diagrams (2.31) are non-trivial. In (2 + 1) dimensions, the MT diagrams contributes by

$$\begin{aligned}
&\tilde{\Pi}_{\text{MT}}^{11}(i\Omega_m) \\
&= \frac{1}{4m^4} \frac{1}{(2\pi)^8} \int d^2 \mathbf{q} d\omega_1 d\omega_2 d^2 \mathbf{k}_1 d^2 \mathbf{k}_2 \mathbf{k}_1 \mathbf{k}_2 (\mathbf{k}_1 + \mathbf{k}_2)_1 (\mathbf{k}_1 + \mathbf{k}_2)_1 G(i\omega_1, \mathbf{k}_1) G(i(\omega_1 + \Omega_m), \mathbf{k}_1) \\
&\quad \times G(i\omega_2, \mathbf{k}_2) G(i(\omega_2 + \Omega_m), \mathbf{k}_2) \cdot D(i(\omega_1 - \omega_2), \mathbf{q}) \\
&= \frac{K^2 v_F^4}{8} \frac{\mathcal{N}^2}{(2\pi)^4} \int d^2 \mathbf{q} d\omega_1 d\omega_2 d\xi_{\mathbf{k}_1} d\xi_{\mathbf{k}_2} \frac{1}{i\frac{\Gamma}{2} \text{sgn}(\omega_1) - \xi_{\mathbf{k}_1}} \frac{1}{i\frac{\Gamma}{2} \text{sgn}(\omega_1 + \Omega_m) - \xi_{\mathbf{k}_1}} \\
&\quad \times \frac{1}{i\frac{\Gamma}{2} \text{sgn}(\omega_2) - \xi_{\mathbf{k}_2}} \frac{1}{i\frac{\Gamma}{2} \text{sgn}(\omega_2 + \Omega_m) - \xi_{\mathbf{k}_2}} \frac{1}{\mathbf{q}^2 + c_0 |\omega_1 - \omega_2|} \\
&= \frac{K^2 v_F^4}{8} \frac{1}{2\pi} \frac{\mathcal{N}^2}{\Gamma^2} \int q dq \int_{-\Omega_m}^0 d\omega_1 \int_{-\Omega_m}^0 d\omega_2 \frac{1}{\mathbf{q}^2 + c_0 |\omega_1 - \omega_2|} \\
&= \frac{K^2 v_F^4 \mathcal{N}^2}{32\pi \Gamma^2} \int_{-\Omega_m}^0 d\omega_1 d\omega_2 \int_{-\Omega_m}^0 \ln \frac{\Lambda_q^2}{c_0 |\omega_1 - \omega_2|} \\
&= \frac{K^2 v_F^4 \mathcal{N}^2}{64\pi \Gamma^2} \Omega_m^2 \ln \left(\frac{e^3 \Lambda_q^4}{c_0^2 |\Omega_m|^2} \right). \tag{2.33}
\end{aligned}$$

Hence the MT diagram correction (2.33) precisely cancels the contribution from electron self-energies (2.30). This does not imply that the boson-electron scattering does not contribute to the resistivity. In fact, up to two loops, there is another polarisation (2.17) to be considered, and this graph is crucial to have the linearity.

Since polarisation (2.17) is generated by $A_\mu a^\mu \psi^\dagger \psi$, it does not exist in [17]. While in [27], the polarisation (2.17) was not considered because it yields a higher order term in frequency. Since the boson propagator (2.14) is dramatically changed, there is no reason to ignore this diagram. In fact, the polarisation (2.17) reads

$$\begin{aligned} & \tilde{\Pi}_{K(3)}^{11}(i\Omega_m) \\ &= \frac{K^2}{2m^2} \mathcal{N}^2 \int d\xi_{\mathbf{k}_1} d\xi_{\mathbf{k}_2} \frac{d^2\mathbf{q}}{(2\pi)^2} \frac{d\omega_1}{2\pi} \frac{d\omega_2}{2\pi} \frac{1}{i\frac{\Gamma}{2}\text{sgn}(\omega_1) - \xi_{\mathbf{k}_1}} \frac{1}{i\frac{\Gamma}{2}\text{sgn}(\omega_2) - \xi_{\mathbf{k}_2}} \frac{1}{\mathbf{q}^2 + c_0|\Omega_m - \omega_1 - \omega_2|} \\ &= \frac{K^2}{16m^2} \frac{\mathcal{N}^2}{2\pi} \Omega_m^2 \left(2 \log \left(\frac{\Lambda_q^4}{c_0^2 \Omega_m^2} \right) - 2 \log \left(\frac{\Lambda^4}{c_0^2} \right) + \log(\Omega_m^2) + 3 - 2i\pi \right). \end{aligned} \quad (2.34)$$

Because we assumed that $A_\mu a^\mu \psi_i^\dagger \psi_j$ is characterised by coupling parameter $\check{K}_{ij}(\mathbf{r})$ satisfying $\langle \check{K}_{ij}(\mathbf{r}) \rangle = 0$ and $\langle \check{K}_{ij}^*(\mathbf{r}) \check{K}_{i'j'}(\mathbf{r}') \rangle = \delta_{ii'} \delta_{jj'} \delta(\mathbf{r} - \mathbf{r}')$, the diagrams such as



$$, \quad (2.35)$$

vanishes, and only diagrams with even number of vertices (of same type) survive in our model. In the model where we would use only K_{ij} not introducing \check{K}_{ij} , then this graph would be non-vanishing. Its contribution would read

$$\begin{aligned} & \tilde{\Pi}_{K(4)}^{11}(i\Omega_m) \\ &= \frac{K^2}{2m^3} \int \frac{d\omega_1}{2\pi} \frac{d\omega_2}{2\pi} \frac{d^2\mathbf{q}}{(2\pi)^2} \frac{d^2\mathbf{k}_1}{(2\pi)^2} \frac{d^2\mathbf{k}_2}{(2\pi)^2} (\mathbf{k}_1)_1 (\mathbf{k}_1 + \mathbf{k}_2)_1 \\ & \quad \times \frac{1}{i\frac{\Gamma}{2}\text{sgn}(\omega_1) - \xi_{\mathbf{k}_1}} \frac{1}{i\frac{\Gamma}{2}\text{sgn}(\omega_1 + \Omega_m) - \xi_{\mathbf{k}_1}} \frac{1}{i\frac{\Gamma}{2}\text{sgn}(\omega_2) - \xi_{\mathbf{k}_2}} \frac{1}{\mathbf{q}^2 + c_0|\omega_1 - \omega_2|} \\ &= \frac{K^2 v_F^2}{32m(2\pi)} \int d\omega_1 d\omega_2 \text{sgn}(\omega_2) \frac{\text{sgn}(\omega_1) - \text{sgn}(\omega_1 + \Omega_m)}{i\frac{\Gamma}{2}\text{sgn}(\omega_1) - i\frac{\Gamma}{2}\text{sgn}(\omega_1 + \Omega_m)} \ln \left(\frac{\Lambda_q^2}{c_0|\omega_1 - \omega_2|} \right) \\ &= -i \frac{K^2 v_F^2}{64m(2\pi)\Gamma} \Omega_m^2 \ln \left(\frac{e^3 \Lambda_q^4}{c_0^2 |\Omega_m|^2} \right). \end{aligned} \quad (2.36)$$

We can see that this term cannot precisely yield linear- T dependence. This is the reason why we introduced \check{K}_{ij} to get rid of the diagram (2.35). Moreover, two-loop correction to fermionic self-energy (2.16) is higher order in frequency. Hence what we compute above is enough to capture the low-temperature feature of the model.

The conductivity $\sigma^{11}(\Omega)$ in *real frequency* Ω can be obtained from the Kubo formula [27, 29]

$$\sigma^{\mu\nu}(\Omega) = -e^2 \frac{\tilde{\Pi}^{\mu\nu}(i\Omega_m \rightarrow \Omega + i0)}{i\Omega}. \quad (2.37)$$

Substituting the first-order polarisation without loop corrections (2.27) into the Kubo formula (2.37), one obtains

$$\sigma_0(\Omega) = \frac{n_e e^2}{m} \frac{1}{\Gamma + i\Omega}, \quad (2.38)$$

which is the usual Drude-like optical conductivity [29]. Taking into account the one-loop corrections to the polarisations from (2.34) one expects the disorder scattering rate Γ will be replaced by the *transport scattering rate* τ_{tr} . To find τ_{tr} , one can focus on the real part of the total conductivity or resistivity, as we are dealing with low frequencies. Substituting the polarisations (2.27), (2.34) into the conductivity (2.37), and taking the real part, one obtains

$$\begin{aligned} \text{Re}\{\sigma(\Omega)\} &= \text{Re}\{\sigma_0(\Omega) + \sigma_K(\Omega)\} \\ &= e^2 \frac{\mathcal{N}v_F^2}{2\Gamma} - \frac{e^2 K^2 \mathcal{N}^2}{16m^2} \frac{1}{2} \Omega, \end{aligned} \quad (2.39)$$

at low frequencies. It is straightforward to find the resistivity

$$\begin{aligned} \text{Re}\left\{\frac{1}{\sigma(\Omega)}\right\} &= \text{Re}\left\{\frac{1}{\sigma_0(\Omega) + \sigma_K(\Omega)}\right\} \\ &\simeq \text{Re}\left\{\frac{1}{\sigma_0(\Omega)}\right\} - \text{Re}\left\{\frac{\sigma_K(\Omega)}{\sigma_0^2(\Omega)}\right\} \\ &= \frac{2}{e^2 \mathcal{N}v_F^2} \left(\Gamma + \frac{K^2 \Gamma^2 \mathcal{N}}{16m^2 v_F^2} |\Omega| \right) \\ &\equiv \frac{m}{n_e e^2} \left(\Gamma + \frac{K^2 \Gamma^2 \mathcal{N}}{16k_F^2} |\Omega| \right). \end{aligned} \quad (2.40)$$

Therefore, one again obtains a linear- T resistivity from an FS coupled to a $U(1)$ gauge field.

According to the calculation in this section, the spatial random disorder can yield linear- T resistivity as well in the model considered in this paper. Comparing the resistivity (2.40) with the one in [17], one finds that they take similar forms, even though both satisfying $\rho = \rho_0 + AT$, with A proportional to the (averaged) square of the coupling parameter between fermions and bosons. However, as we have seen above, the linear resistivity in our model is from $A_\mu a^\mu \psi^\dagger \psi$ instead of $\mathbf{a} \psi^\dagger \nabla \psi$, which is a fundamental difference with the one studied in [17]. We could expect that because of the scaling dimension of the vector is one higher than that of the scalar so that two different type of interaction could generate the same temperature scaling. In the following section, we will generalise the system to $(3+1)$ dimensions and illustrate that the transport properties are indeed independent of the boson type, such that a QED-like interaction and a Yukawa-like interaction will share the same qualitative properties. However, we will find that the resistivity is no longer linear in temperature in higher spatial dimensions because *the scaling dimension of fields crucially depends on the dimensionality of spacetime*.

Difference between vector model and scalar model Though the vector model in this article also yields a linear resistivity, the computation is rather different with the scalar (Yukawa) model in [17]. In spatially random Yukawa theory, the linearity comes from fermionic self-energy (2.29). The vertex correction including MT diagram and AL digrams is zero due to the symmetry of integrand. In contrast, our vector model is characterised by the vertex $\psi^\dagger \mathbf{a} \nabla \psi$, each of which contains a factor of $(k_1 + k_2)$. Therefore, graphs such as MT diagram (2.31) do not necessary vanish. Unlike the spatially random Yukawa theory [17], the vector model in this article can receive higher-order corrections to the linearity. It has been illustrated that MT graph (2.31) precisely cancels the contribution from self-energy (2.29). Instead, the key to linear- T resistivity in a vector model is the coupling $A_\mu a_\mu \psi^\dagger \psi$, graphically represented by (2.17). Consequently, the coefficient of T takes a basically different form to the one in [17].

Difference between vector models with and without spatial randomness There are also important differences between our model with normal FS-gauge coupling model studied in [27]. First of all, because the coupling parameter has zero expectation value in this article, only diagrams with even number of same vertices are non-vanishing. Therefore, the number of diagrams are reduced in our theory. More importantly, in [27] the coupling $A_\mu a_\mu \psi^\dagger \psi$ results in a higher-order term, so it is neglected. One thus obtains a would-be $T^{4/3}$ resistivity from self-energies with vertex $\psi^\dagger \mathbf{a} \nabla \psi$. On the other hand, we find that the diagram (2.17) is not of higher-order once impurity and spatial randomness are imposed, which means that they should be taken into account. Due to the cancellation between self-energy term (2.29) and MT graph (2.31), the only non-trivial contribution is from (2.17). In other words, the T -dependence in our case is a result of $A_\mu a_\mu \psi^\dagger \psi$, instead of $\psi^\dagger \mathbf{a} \nabla \psi$.

3 Breakdown of Linear-T Resistivity in Higher Dimensions

One of our interest is to see whether the mechanism of SYK-like randomization works in dimension other than two. Hence we want to study the model in higher dimensions. Although most of the unconventional superconductors and their strange-metal regimes are observed in $(2 + 1)$ dimensional systems, yet there are examples of $3D$ superconductor showing that linear- T behaviour in their normal phase [39] so that one might expect that the linearity be independent of dimensionality [40]. Therefore this offers a non-trivial test of such conjecture and this will also test whether SYK-rization always bestows the linear- T resistivity even in higher dimensions and help us to understand the underlying mechanics of strange metal.

It turns out that the random disorder with spatial dependence loses its power in higher dimensions. This happens not only in the model considered in this paper, but also in the model discussed in [17]. However, we will find that these two systems, share the same temperature dependence in the transport, which supports the result in section 2.

3.1 Three dimensional Fermi surface coupled with gauge field

Generalised the model (2.1) to (3 + 1) dimensions, the $U(1)$ gauge field has two degrees of freedom. Let 1 and 2 be the directions perpendicular to \mathbf{q} , and one obtains a similar $G - \Sigma$ theory with saddle point equation yielding the propagators as well as self-energies,

$$G = G_* = (-\partial_\tau - \varepsilon_k + \mu - \Sigma)^{-1} \quad (3.1)$$

$$\Sigma = \Sigma_* = v^2 G(\tau, \mathbf{r}) \delta^3(\mathbf{r}) + \frac{1}{m^2} \frac{(k_1 + k_2)^a}{2} \frac{(k_1 + k_2)^b}{2} D_{ab} G \bar{\delta} + \frac{1}{4m^2} D_{\mu\nu} D^{\mu\nu} G \bar{\delta} \quad (3.2)$$

$$D_{ab} = D_{*ab} = K^2 (-(-\partial_\tau^2 + \mathbf{q}^2) g^{ab} - K^2 \Pi^{ab})^{-1} \quad (3.3)$$

$$\Pi_{ab} = \Pi_{*ab} = -\frac{1}{m^2} \frac{(k_1 + k_2)_a}{2} \frac{(k_1 + k_2)_b}{2} G \bar{\delta} \cdot G - \frac{1}{4m^2} G D_{ab} G \bar{\delta}, \quad (3.4)$$

where $a, b = 1, 2$.

Repeating the computation in section 2, one can first find the fermionic self-energy

$$\begin{aligned} \Sigma_v(i\omega_n) &= v^2 \int \frac{d^3 \mathbf{k}'}{(2\pi)^3} G(i\omega_n, \mathbf{k}') \\ &= v^2 \int \mathcal{N} d\xi_{\mathbf{k}'} \frac{1}{i\omega_n - \xi_{\mathbf{k}'} - \Sigma(i\omega_n, \mathbf{k}')} \\ &= -i \frac{\Gamma}{2} \text{sgn}(\omega_n), \end{aligned} \quad (3.5)$$

where $\Gamma \equiv 2\pi v^2 \mathcal{N}$ is again the disorder scattering rate, and $\mathcal{N} = m^{3/2} \sqrt{\varepsilon_{\mathbf{k}_F}} / (2\pi^2)$ is the DoS at the Fermi energy in three dimensions. This will bring a constant residue resistivity, which is basically the same with (2 + 1)-dimensional case in the presence of an FS.

Then the dominant part of polarisation is

$$\begin{aligned} &\tilde{\Pi}_0^{ab}(i\Omega_m) \\ &= \frac{1}{m^2} \mathcal{N} \int \frac{d\omega_n}{2\pi} \int d\xi_{\mathbf{k}} \frac{k^a k^b}{i \frac{\Gamma}{2} \text{sgn}(\omega_n) - \xi_{\mathbf{k}}} \left(\frac{1}{i \frac{\Gamma}{2} \text{sgn}(\omega_n + \Omega_m) - \xi_{\mathbf{k}}} - \frac{1}{i \frac{\Gamma}{2} \text{sgn}(\omega_n) - \xi_{\mathbf{k}}} \right) \\ &= \frac{v_F^2}{3} \delta^{ab} \mathcal{N} \frac{1}{\Gamma} |\Omega_m|, \end{aligned} \quad (3.6)$$

where we impose the isotropy such that the conductivity is diagonal.

Similarly, one obtains the bosonic self-energy

$$\begin{aligned} &-K^2 \Pi_0^{ab}(i\Omega_m) \\ &= \frac{K^2}{6m^2} \mathcal{N}^2 \int \frac{d\omega_n}{2\pi} \int d\xi_{\mathbf{k}} d\xi_{\mathbf{k}'} \frac{k_F^2 \delta^{ab}}{i \frac{\Gamma}{2} \text{sgn}(\omega_n) - \xi_{\mathbf{k}}} \left(\frac{1}{i \frac{\Gamma}{2} \text{sgn}(\omega_n + \Omega_m) - \xi_{\mathbf{k}'}} - \frac{1}{i \frac{\Gamma}{2} \text{sgn}(\omega_n) - \xi_{\mathbf{k}'}} \right) \\ &= \pi \mathcal{N}^2 K^2 \frac{v_F^2}{12} |\Omega_m| \delta^{ab} \\ &\equiv c_0 \delta^{ab} |\Omega_m|. \end{aligned} \quad (3.7)$$

Assume

$$D_{ab} = K^2(-(-\partial_\tau^2 + \mathbf{q}^2)g^{ab} - K^2\Pi^{ab})^{-1} = -\frac{g_{ab}K^2}{(-\partial_\tau^2 + \mathbf{q}^2)(1 + \Pi)}. \quad (3.8)$$

By requiring

$$-\frac{g_{ab}}{(-\partial_\tau^2 + \mathbf{q}^2)(1 + \Pi)}(-(-\partial_\tau^2 + \mathbf{q}^2)g^{bc} - K^2\Pi^{bc}\bar{\delta}) = \delta_a^c, \quad (3.9)$$

one finds

$$\Pi = \frac{c_0|\Omega_m|}{-\partial_\tau^2 + \mathbf{q}^2}, \quad (3.10)$$

so

$$D_{ab}(i\Omega_m) = -\frac{g_{ab}K^2}{-\partial_\tau^2 + \mathbf{q}^2 + c_0|\Omega_m|}, \quad (3.11)$$

which is the same in form with vector propagator in $(2 + 1)$ dimensions.

This will then give us the fermionic self-energies from the electron-boson coupling,

$$\begin{aligned} \Sigma_K(i\omega_n) &= \frac{K^2 k_F^2}{6m^2} \mathcal{N} \int \frac{d\Omega_m}{2\pi} \int \frac{d^3\mathbf{q}}{(2\pi)^3} d\xi_{\mathbf{k}} \frac{1}{i\frac{\Gamma}{2}\text{sgn}(\omega_n + \Omega_m) - \xi_{\mathbf{k}}} \frac{1}{\mathbf{q}^2 + c_0|\Omega_m|} \\ &= -i \frac{K^2 v_F^2}{6} \mathcal{N} \int_{-\infty}^{+\infty} d\Omega_m \int_0^{\Lambda_q} \frac{4\pi|\mathbf{q}|^2 d|\mathbf{q}|}{(2\pi)^3} \text{sgn}(\omega_n + \Omega_m) \frac{1}{|\mathbf{q}|^2 + c_0|\Omega_m|} \\ &= -i \frac{K^2 v_F^2}{12\pi^2} \mathcal{N} \int d\Omega_m \text{sgn}(\omega_n + \Omega_m) \left(\Lambda_q - \frac{\sqrt{c_0|\Omega_m|}\pi}{2} \right) \\ &= i \frac{K^2 v_F^2}{18\pi} \mathcal{N} \sqrt{c_0} |\omega_n|^{3/2}, \end{aligned} \quad (3.12)$$

where Λ_q is a UV cut-off on q . One finds that the specific heat no longer takes a form of $\omega \ln(1/\omega)$, and the linear- T resistivity is not expected to exist any more. To be more explicit, let us continue to the polarisation at the next order, which reads

$$\begin{aligned} &2\tilde{\Pi}_{K(1)}^{ab}(i\Omega_m) \\ &= 2 \frac{1}{m^2} \mathcal{N} \int \frac{d\omega_n}{2\pi} \int d\xi_{\mathbf{k}} k^a k^b \left(\frac{1}{i\frac{\Gamma}{2}\text{sgn}(\omega_n) - \xi_{\mathbf{k}}} \right)^2 \frac{1}{i\frac{\Gamma}{2}\text{sgn}(\omega_n + \Omega_m) - \xi_{\mathbf{k}}} \Sigma_K(i\omega_n) \Big|_{\Omega_m=0} \\ &= i \frac{K^2}{3} v_F^2 \delta^{ab} \mathcal{N} \int d\omega_n \frac{-\text{sgn}(\omega_n + \Omega_m) + \text{sgn}(\omega_n)}{(i\frac{\Gamma}{2}\text{sgn}(\omega_n + \Omega_m) - i\frac{\Gamma}{2}\text{sgn}(\omega_n))^2} \left[i \frac{v_F^2}{18\pi} \mathcal{N} \sqrt{c_0} |\omega_n|^{3/2} \right] \\ &= \frac{1}{135\pi} K^2 v_F^4 \delta^{ab} \frac{\mathcal{N}^2}{\Gamma^2} \sqrt{c_0} |\Omega_m|^{5/2}. \end{aligned} \quad (3.13)$$

The vertex correction from MT diagrams reads

$$\begin{aligned}
& \tilde{\Pi}_{\text{MT}}^{ab}(i\Omega_m) \\
&= \frac{1}{4m^4} \frac{1}{(2\pi)^{11}} \int d^3\mathbf{q} d\omega_1 d\omega_2 d^3\mathbf{k}_1 d^3\mathbf{k}_2 (\mathbf{k}_1)^a (\mathbf{k}_2)^b (\mathbf{k}_1 + \mathbf{k}_2)_{a'} (\mathbf{k}_1 + \mathbf{k}_2)_{b'} G(i\omega_1, \mathbf{k}_1) G(i(\omega_1 + \Omega_m), \mathbf{k}_1) \\
&\quad \times G(i\omega_2, \mathbf{k}_2) G(i(\omega_2 + \Omega_m), \mathbf{k}_2) \cdot D^{a'b'}(i(\omega_1 - \omega_2), \mathbf{q}) \\
&= \frac{K^2 v_F^4 \mathcal{N}^2}{18 (2\pi)^5} \int d^3\mathbf{q} d\omega_1 d\omega_2 d\xi_{\mathbf{k}_1} d\xi_{\mathbf{k}_2} \frac{1}{i\frac{\Gamma}{2}\text{sgn}(\omega_1) - \xi_{\mathbf{k}_1}} \frac{1}{i\frac{\Gamma}{2}\text{sgn}(\omega_1 + \Omega_m) - \xi_{\mathbf{k}_1}} \\
&\quad \times \frac{1}{i\frac{\Gamma}{2}\text{sgn}(\omega_2) - \xi_{\mathbf{k}_2}} \frac{1}{i\frac{\Gamma}{2}\text{sgn}(\omega_2 + \Omega_m) - \xi_{\mathbf{k}_2}} \frac{1}{\mathbf{q}^2 + c_0|\omega_1 - \omega_2|} \\
&= -\delta^{ab} \frac{K^2 v_F^4 \mathcal{N}^2}{135\pi\Gamma^2} \Omega_m^2 \left(\Lambda_q - \sqrt{c_0}|\Omega|^{3/2} \right), \tag{3.14}
\end{aligned}$$

cancelling again the self-energy contribution (3.13) after taking the real part of the conductivity. The non-trivial temperature dependence thus comes from the two-loop polarisation (2.17), which reads

$$\begin{aligned}
& \tilde{\Pi}_{K(3)}^{ab}(i\Omega_m) \\
&= \delta^{ab} \frac{K^2}{4m^2} \mathcal{N}^2 \int d\xi_{\mathbf{k}_1} d\xi_{\mathbf{k}_2} \frac{d^3\mathbf{q}}{(2\pi)^3} \frac{d\omega_1}{2\pi} \frac{d\omega_2}{2\pi} \frac{1}{i\frac{\Gamma}{2}\text{sgn}(\omega_1) - \xi_{\mathbf{k}_1}} \frac{1}{i\frac{\Gamma}{2}\text{sgn}(\omega_2) - \xi_{\mathbf{k}_2}} \frac{1}{\mathbf{q}^2 + c_0|\Omega_m - \omega_1 - \omega_2|} \\
&= -\delta^{ab} \frac{K^2}{16m^2} \frac{\mathcal{N}^2}{2\pi^2} \int d\omega_1 d\omega_2 \text{sgn}(\omega_1) \text{sgn}(\omega_2) \left(\Lambda_q - \frac{\pi\sqrt{c_0}}{2} \sqrt{|\Omega - \omega_1 - \omega_2|} \right) \\
&= \delta^{ab} \frac{K^2}{16m^2} \frac{\mathcal{N}^2}{2\pi^2} \Omega_m^2 \left(\frac{\Lambda_q}{2} - \frac{2}{15} \sqrt{c_0} \pi |\Omega_m|^{1/2} \right). \tag{3.15}
\end{aligned}$$

Similarly, if we take $\tilde{K}_{ij} = K_{ij}$, the graph (2.35) will yield a polarisation

$$\begin{aligned}
& \tilde{\Pi}_{K(4)}^{ab}(i\Omega_m) \\
&= \frac{K^2}{2m^3} \int \frac{d\omega_1}{2\pi} \frac{d\omega_2}{2\pi} \frac{d^3\mathbf{q}}{(2\pi)^3} \frac{d^3\mathbf{k}_1}{(2\pi)^3} \frac{d^3\mathbf{k}_2}{(2\pi)^3} (\mathbf{k}_1)^a (\mathbf{k}_1 + \mathbf{k}_2)^b \frac{1}{i\frac{\Gamma}{2}\text{sgn}(\omega_1) - \xi_{\mathbf{k}_1}} \frac{1}{i\frac{\Gamma}{2}\text{sgn}(\omega_1 + \Omega_m) - \xi_{\mathbf{k}_1}} \\
&\quad \times \frac{1}{i\frac{\Gamma}{2}\text{sgn}(\omega_2) - \xi_{\mathbf{k}_2}} \frac{1}{\mathbf{q}^2 + c_0|\omega_1 - \omega_2|} \\
&= \frac{\delta^{ab} K^2 v_F^2}{48m\pi^2} \int d\omega_1 d\omega_2 \text{sgn}(\omega_2) \frac{\text{sgn}(\omega_1) - \text{sgn}(\omega_1 + \Omega_m)}{i\frac{\Gamma}{2}\text{sgn}(\omega_1) - i\frac{\Gamma}{2}\text{sgn}(\omega_1 + \Omega_m)} \left(\Lambda_q - \sqrt{c_0}|\omega_1 - \omega_2| \frac{\pi}{2} \right) \\
&= -i\delta^{ab} \frac{K^2 v_F^2}{96\pi\Gamma} \Omega_m^2 \frac{2}{5} \Omega_m^{5/2}. \tag{3.16}
\end{aligned}$$

Using Kubo formula (2.37), one finds

$$\text{Re}\left\{ \sigma_K^{ab} \right\} \propto \delta^{ab} \Omega_m^{3/2}. \tag{3.17}$$

Therefore, there is no linear- T resistivity after the model (2.8) is generalised to higher dimensions. Similarly, we find that the spatially random Yukawa model in [17] also lose linear- T resistivity in $(3+1)$ dimensions.

3.2 Random Yukawa coupling model in 3+1 dimension

This subsection provides a straightforward generalisation of the random Yukawa model of ref. [17] and illustrates the nonlinear- T resistivity. As the spatially uniform theory (described by g -coupling in [17]) has no contribution to the resistivity due to the cancellation from vertex corrections [17], we will only consider the potential disorder and interaction disorder. For simplicity, let us relabel the parameter g' in [17] by g . Therefore, the action is

$$\begin{aligned}
\mathcal{S}_g &= \int d\tau \sum_{\mathbf{k}} \sum_{i=1}^N \psi_{i\mathbf{k}}^\dagger(\tau) [\partial_\tau + \varepsilon(\mathbf{k})] \psi_{i\mathbf{k}}(\tau) \\
&+ \frac{1}{2} \int d\tau \sum_{\mathbf{q}} \sum_{i=1}^N \phi_{i\mathbf{q}}(\tau) [-\partial_\tau^2 + \mathbf{q}^2 + m_b^2] \phi_{i,-\mathbf{q}}(\tau) \\
&+ \frac{1}{N} \int d\tau d^3r \sum_{i,j,l=1}^N g_{ijl}(\mathbf{r}) \psi_i^\dagger(\mathbf{r}, \tau) \psi_j(\mathbf{r}, \tau) \phi_l(\mathbf{r}, \tau) \\
&+ \frac{1}{\sqrt{N}} \int d^3r d\tau v_{ij}(\mathbf{r}) \psi_i^\dagger(\mathbf{r}, \tau) \psi_j(\mathbf{r}, \tau), \tag{3.18}
\end{aligned}$$

where the random coupling g_{ijk} and v_{ij} has zero mean and

$$\begin{aligned}
\langle v_{ij}^*(\mathbf{r}) v_{i'j'}(\mathbf{r}') \rangle &= v^2 \delta_{ii'} \delta_{jj'} \delta(\mathbf{r} - \mathbf{r}'), \\
\langle g_{ijl}^*(\mathbf{r}) g_{i'j'l'}(\mathbf{r}') \rangle &= g^2 \delta_{ii'} \delta_{jj'} \delta_{ll'} \delta(\mathbf{r} - \mathbf{r}'). \tag{3.19}
\end{aligned}$$

After performing the disorder average and introducing self-energies as dynamical degrees of freedom, one obtains the saddle point equations

$$\begin{aligned}
\Sigma(\tau, \mathbf{r}) &= v^2 G(\tau, \mathbf{r} = 0) \delta^2(\mathbf{r}) + g^2 G(\tau, \mathbf{r} = 0) D(\tau, \mathbf{r} = 0) \delta^2(\mathbf{r}) \\
\Pi(\tau, \mathbf{r}) &= -g^2 G(-\tau, \mathbf{r} = 0) G(\tau, \mathbf{r} = 0) \delta^2(\mathbf{r}) \\
G(i\omega_n, \mathbf{k}) &= \frac{1}{i\omega_n - \varepsilon_{\mathbf{k}} + \mu - \Sigma(i\omega_n, \mathbf{k})} \\
D(i\Omega_m, \mathbf{q}) &= \frac{1}{\Omega_m^2 + \mathbf{q}^2 + m_b^2 - \Pi(i\Omega_m, \mathbf{q})}. \tag{3.20}
\end{aligned}$$

These take the same form with those for (2 + 1) dimensions [17].

Similarly, one calculate first the self-energy from potential disorder,

$$\begin{aligned}
\Sigma_v(i\omega_n, \mathbf{k}) &= v^2 \int \mathcal{N} d\xi_{\mathbf{q}} \frac{1}{i\omega_n - \xi_{\mathbf{q}} - \Sigma(i\omega_n, \mathbf{q})} \\
&= -i \frac{\Gamma}{2} \text{sgn}(\omega_n), \tag{3.21}
\end{aligned}$$

where $\Gamma = 2\pi v^2 \mathcal{N}$ and \mathcal{N} is the DoS at FS in three dimensions. Since Γ is the largest scale in this system, the Fermionic propagator can be approximated into

$$G(i\omega_n, \mathbf{k}) \simeq \frac{1}{i \frac{\Gamma}{2} \text{sgn}(\omega_n) - \xi_{\mathbf{k}}} \tag{3.22}$$

at low frequencies.

Then, continuing to the bosonic self-energies, we obtains

$$\begin{aligned}
& \Pi_g(i\Omega_m) \\
&= -g^2 \mathcal{N}^2 \int \frac{d\omega_n}{2\pi} \int d\xi_{\mathbf{k}} d\xi_{\mathbf{k}'} \frac{1}{i\frac{\Gamma}{2} \text{sgn}(\omega_n) - \xi_{\mathbf{k}}} \left(\frac{1}{i\frac{\Gamma}{2} \text{sgn}(\omega_n + \Omega_m) - \xi_{\mathbf{k}'}} - \frac{1}{i\frac{\Gamma}{2} \text{sgn}(\omega_n) - \xi_{\mathbf{k}'}} \right) \\
&= \frac{i}{2} g^2 \mathcal{N}^2 \int d\omega_n \int d\xi_{\mathbf{k}'} \text{sgn}(\omega_n) \left(\frac{1}{i\frac{\Gamma}{2} \text{sgn}(\omega_n + \Omega_m) - \xi_{\mathbf{k}'}} - \frac{1}{i\frac{\Gamma}{2} \text{sgn}(\omega_n) - \xi_{\mathbf{k}'}} \right) \\
&= \frac{\pi}{2} g^2 \mathcal{N}^2 \int d\omega_n \text{sgn}(\omega_n) (\text{sgn}(\omega_n + \Omega_m) - \text{sgn}(\omega_n)) \\
&= -\pi \mathcal{N}^2 g^2 |\Omega_m| \\
&\equiv -c_d |\Omega_m|. \tag{3.23}
\end{aligned}$$

One can use the result above to find the self-energy from random Yukawa coupling, which reads

$$\begin{aligned}
\Sigma_g(i\omega_n) &= g^2 \mathcal{N} \int_{-\infty}^{+\infty} \frac{d\Omega_m}{2\pi} \int d\xi_{\mathbf{k}} \int_0^{+\infty} \frac{q^2 dq}{2\pi^2} \frac{1}{i\frac{\Gamma}{2} \text{sgn}(\omega_n + \Omega_m) - \xi_{\mathbf{k}}} \frac{1}{q^2 + c_d |\Omega_m|} \\
&= -ig^2 \mathcal{N} \int_{-\infty}^{+\infty} d\Omega_m \int_0^{+\infty} \frac{q^2 dq}{4\pi^2} \text{sgn}(\omega_n + \Omega_m) \frac{1}{q^2 + c_d |\Omega_m|} \\
&= \frac{-ig^2}{4\pi^2} \mathcal{N} \int_{-\infty}^{+\infty} d\Omega_m \left(\Lambda_q - \frac{\pi}{2} \sqrt{c_d |\Omega_m|} \right) \text{sgn}(\omega_n + \Omega_m) \\
&= \frac{ig^2}{6\pi} \mathcal{N} |\omega_n|^{3/2}. \tag{3.24}
\end{aligned}$$

We find that $T \ln(1/T)$ term no longer exist either, and there should be no linear- T resistivity. To be explicit, let us compute the conductivity and see how the dimension changes the result. The derivation of conductivity in [18] is still valid, so one can directly move on to the computation.

First is the first-order current-current correlation dominated by potential disorder,

$$\begin{aligned}
\frac{1}{N} \tilde{\Pi}_v^{xx}(i\Omega_m) &= v_F^2 \mathcal{N} \int_{-\pi}^{\pi} d\theta \cos^2(\theta) \int \frac{d\omega_n}{2\pi} \int d\xi_{\mathbf{k}} \frac{1}{i\frac{\Gamma}{2} \text{sgn}(\omega_n) - \xi_{\mathbf{k}}} \frac{1}{i\frac{\Gamma}{2} \text{sgn}(\omega_n + \Omega_m) - \xi_{\mathbf{k}}} \\
&= \frac{\mathcal{N} v_F^2}{2\Gamma} \Omega_m. \tag{3.25}
\end{aligned}$$

So the conductivity is

$$\frac{1}{N} \text{Re}[\sigma_{\Sigma, v}] = -\frac{1}{N} \frac{\text{Im}[\Pi_v^{xx}(i\Omega_m) - \Pi_v^{xx}(0)|_{i\Omega_m \rightarrow \Omega + i0^+}]}{\Omega} = \frac{\mathcal{N} v_F^2}{2\Gamma}, \tag{3.26}$$

which is a constant, qualitatively the same with $(2+1)$ dimensional model in [17].

Then the contribution from g term is

$$\begin{aligned}
& \frac{1}{N} \tilde{\Pi}_g^{xx}(i\Omega_m) \\
&= 2v_F^2 \mathcal{N} \int_{-\infty}^{+\infty} \frac{d\omega'_n}{2\pi} \int_{-\pi}^{+\pi} \frac{d\theta \cos^2 \theta}{2\pi} \int_{-\infty}^{\infty} d\xi_{\mathbf{k}} \frac{1}{i\frac{\Gamma}{2} \text{sgn}(\Omega_m + \omega'_n) - \xi_{\mathbf{k}}} \frac{1}{(i\frac{\Gamma}{2} \text{sgn}(\omega'_n) - \xi_{\mathbf{k}})^2} \Sigma_g(i\Omega_m) \\
&= \frac{i}{2} v_F^2 \mathcal{N} \int_{-\infty}^{+\infty} d\omega'_n \frac{-\text{sgn}(\omega'_n + \Omega_m) + \text{sgn}(\omega'_n)}{(i\frac{\Gamma}{2} \text{sgn}(\Omega_m + \omega'_n) - i\frac{\Gamma}{2} \text{sgn}(\omega'_n))^2} \left(\frac{ig^2}{6\pi} \mathcal{N} |\omega_n|^{3/2} \right) \\
&= -\frac{v_F^2}{30\pi} \frac{\mathcal{N}^2 g^2}{\Gamma^2} |\Omega_m|^{5/2}. \tag{3.27}
\end{aligned}$$

Similarly, the analytic continuation to the real axis bring us a conductivity $\propto \Omega^{3/2}$.

It is not surprising that the linear- T resistivity from spatial random coupling cannot survive in higher dimensions. Let us close this section with a rough analysis and take the spatial random coupling model in this paper together with the spatially random Yukawa model [17] for example.

As vertex corrections vanish, the non-trivial Ω - (or T -) dependence comes from the one-loop corrections to the polarisation



$$\tag{3.28}$$

The qualitative behaviour can be conveniently read from the electron self-energy



$$\tag{3.29}$$

Because the momentum conservation is removed on each vertex, the dependence on frequency or temperature is from the integral

$$\int d\Omega_m \int d^d \mathbf{q} \int d\xi_{\mathbf{k}} \frac{1}{i\frac{\Gamma}{2} \text{sgn}(\omega_n + \Omega_m) - \xi_{\mathbf{k}}} \frac{1}{\mathbf{q}^2 + c|\Omega_m|} \tag{3.30}$$

in $(d+1)$ dimensions with c a constant. $d\Omega_m$ will produce a term linear in frequency, while $\int d\xi_{\mathbf{k}}$ yields a term of $\mathcal{O}(\omega^0)$. The integral over \mathbf{q} in general will bring a term with dimension of $\omega^{(d-2)/2}$. As a consequence, only when $d=2$, can these models bring us a linear- T dependence.

Similarly, the non-trivial T -dependence is from polarisation (2.17), which is proportional to

$$\begin{aligned}
& \int d\omega_1 d\omega_2 \int d^d \mathbf{q} \int d\xi_{\mathbf{k}_1} d\xi_{\mathbf{k}_2} \frac{1}{i\frac{\Gamma}{2} \text{sgn}(\omega_1) - \xi_{\mathbf{k}_1}} \frac{1}{i\frac{\Gamma}{2} \text{sgn}(\omega_2) - \xi_{\mathbf{k}_2}} \frac{1}{\mathbf{q}^2 + c|\Omega_m - \omega_1 - \omega_2|} \\
& \sim \Omega_m^{(d+2)/2}. \tag{3.31}
\end{aligned}$$

The Kubo formula then yields a resistivity $\sim T^{d/2}$, so only when $d = 2$ can we have linearity.

Therefore, the idea of random spatial Yukawa type interaction to obtain a resistivity linear in temperature in [17–19] works only in (2+1) dimensions [24]. Comparing the result of scalar boson (3.27) with that of vector boson (3.13), one finds that they take the similar form, implying that the effects of spatial random coupling to the resistivity is independent of the type of bosons.

4 The Emergence of Linearity: Fermi Liquid vs Strange Metal

So far, we have shown that boson-electron scattering can be a source of linear resistivity, in spite of the boson types. To show the linearity, the ref. [17] and this article did much calculation. We found that different Feynman diagrams are used to get the same qualitative property. Our purpose here is that the qualitative properties can be read directly without cumbersome computation. We will follow Bloch’s argument [41–43] to give an intuitive understanding of this linear resistivity and its dimensional dependence.

First of all, the scattering rate contains contribution from DoS and a small-angle correction $(1 - \cos \theta)$, with θ the scattering angle, such that the total transport rate is

$$\rho \sim \frac{1}{\tau_{\text{tr}}} \sim \int \text{DoS} \cdot (1 - \cos \theta). \quad (4.1)$$

We will use eqn.(4.1) to see what models have linear in T dependence and why it is difficult to obtain.

Fermi Liquid ($\sim T^2$) Let us start with the Fermi liquid theory which is characterized by the T^2 resistivity. The quadratic behaviour originates from collisions among quasiparticles. The simplest model is the binary collision by the 4-fermion interaction term, $u\psi^\dagger\psi^\dagger\psi\psi$ [29, 44]. Two particles with momentum \mathbf{k}_1 and \mathbf{k}_2 scatter into \mathbf{k}'_1 and \mathbf{k}'_2 ,

$$\mathbf{k}_1 + \mathbf{k}_2 \rightarrow \mathbf{k}'_1 + \mathbf{k}'_2, \quad (4.2)$$

as is shown in Fig. 1.

This process can also be viewed as the decay of one quasi-particle into two quasi-particles and one quasi-hole so that the scattering rate can be calculated as the decay rate of particle 1 using the Fermi’s golden rule [29, 32]:

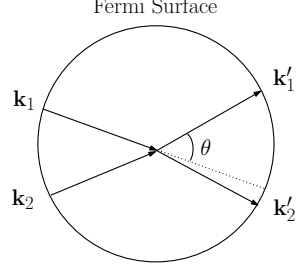


Figure 1. An illustration of a binary quasiparticle collision.

$$\begin{aligned}
\rho &\sim \int d\mathbf{k}_2 d\mathbf{k}'_1 d\mathbf{k}'_2 \delta(\mathbf{k}_1 + \mathbf{k}_2 - \mathbf{k}'_1 - \mathbf{k}'_2) \delta(\epsilon_1 + \epsilon_2 - \epsilon'_1 - \epsilon'_2) (1 - \cos \theta) f_{\mathbf{k}_2} (1 - f_{\mathbf{k}'_1}) (1 - f_{\mathbf{k}'_2}) \\
&= \int d\mathbf{k}'_1 d\mathbf{k}'_2 \delta(\epsilon_1 + \epsilon_2 - \epsilon'_1 - \epsilon'_2) (1 - \cos \theta) f_{\mathbf{k}'_1 + \mathbf{k}'_2 - \mathbf{k}_1} (1 - f_{\mathbf{k}'_1}) (1 - f_{\mathbf{k}'_2}) \\
&\propto \int d\epsilon'_1 d\epsilon'_2 f(-\epsilon'_1) f(-\epsilon'_2) f(\epsilon'_1 + \epsilon'_2 - \epsilon_1) \\
&\sim T^2 \int dx dy \frac{1}{1 - e^{-x}} \frac{1}{1 - e^{-y}} \frac{1}{1 - e^z}, \tag{4.3}
\end{aligned}$$

where $f_{\mathbf{k}}$ is the Fermi function. The essential steps for the T^2 is followings: i) step 1. the momentum conservation reduces one momentum integral and the energy conservation and distribution functions restrict the integration range around the Fermi surface (FS). ii) step 2. we split momentum integral into radial and angular directions: $d^d \mathbf{k} \sim D_d(\epsilon) d\epsilon d\Omega$ where $D_d(\epsilon) = \epsilon^{(d-2)/2} \sim \epsilon_F^{(d-2)/2} \sim \text{constant}$ due to the FS restriction. iii) step 3. the angular integral does not contribute to the temperature scaling so that the momentum integration is reduced to the energy integral. vi) step 4. $x \equiv \epsilon'_1 \beta$, $y \equiv \epsilon'_2 \beta$, and $z \equiv \epsilon_2 \beta$, with $\beta \equiv 1/(k_B T)$.

Therefore, the T^2 resistivity comes merely from DoS of fermions in Fermi liquids. In all these steps, the presence of the FS is essential and this result is true in all dimensions. Notice, however, that to get the constant piece of the resistivity, this 4-fermi interaction model should also introduce the random disorder potential term.

Yukawa Coupling ($\sim T^2$) A similar quadratic resistivity can also be generated from electron-boson scattering with a random Yukawa coupling $g_{ijl} \psi_i^\dagger \psi_j \phi_l$ [18] and a spatial disorder potential $v_{ij}(\mathbf{r}) \psi_i^\dagger \psi_j$ ². In most cases, in addition to the electronic self-energies graphs in (2.29), we also have to include the vertex corrections given by the MT diagram

Although the self-energy (2.29) brings a resistivity linear in T [17, 18], this linear dependence is canceled by the MT graph (2.31), so that one has to go to the next order given by the AL diagrams in (2.32), which result in the resistivity $\rho \sim T^2$. Since it does not involve the the random Yukawa coupling it can be considered as a model for the Fermi

²Appendix A shows that the flavour disorder hardly changes the qualitative properties.

liquid. A limitation of this model is that it works only in $(2 + 1)$ dimension.

Strange metal from the Spatially Random Yukawa Coupling On the other hand, the space dependent random coupling of vector-fermion in this paper as well as the scalar-fermion model in [17] receive no vertex corrections so that the term which is linear in T survives. To see the reason, let us take MT diagram (2.31) for example. Usually its contribution reads

$$\int d\omega_1 d\omega_2 d\mathbf{k}_1 d\mathbf{k}_2 \mathbf{k}_1 \mathbf{k}_2 G(i\omega_1, \mathbf{k}_1) G(i(\omega_1 + \Omega_m), \mathbf{k}_1) \times G(i\omega_2, \mathbf{k}_2) G(i(\omega_2 + \Omega_m), \mathbf{k}_2) D(i(\omega_1 - \omega_2), \mathbf{k}_1 - \mathbf{k}_2). \quad (4.4)$$

Notice that the delta function correlation of the spatial random coupling implies that the vertices w and w' in (2.31) should be contracted. After the contraction of vertex w and w' in a electronic self-energy diagram, the bosonic propagator becomes a loop, as illustrated below,



The diagram illustrates the contraction of two vertices, w and w' , which are connected by a dashed line. An arrow points to the resulting structure, which is a loop (a circle) with a wavy line (representing a boson) attached to it, and a solid line (representing a fermion) connecting the two vertices w and w' through the loop.

This means that the momentum conservation imposed on the vertices is relaxed and the bosonic momentum \mathbf{q} is decoupled from the fermion momentum \mathbf{k} so that the integral (4.4) becomes

$$\int d\omega_1 d\omega_2 d\mathbf{k}_1 d\mathbf{k}_2 d\mathbf{q} \mathbf{k}_1 \mathbf{k}_2 G(i\omega_1, \mathbf{k}_1) G(i(\omega_1 + \Omega_m), \mathbf{k}_1) \times G(i\omega_2, \mathbf{k}_2) G(i(\omega_2 + \Omega_m), \mathbf{k}_2) \cdot D(i(\omega_1 - \omega_2), \mathbf{q}). \quad (4.6)$$

Now notice that the integrand is an odd function of \mathbf{k}_1 and \mathbf{k}_2 since G 's are even functions, so that the diagram vanishes [17]. Similarly all AL diagrams vanish, and as the consequence, the self-energy given by (2.29) survives and the resistivity is linear- T .

Strange metal from Spatially Random Gauge Field Coupling In this paper, we consider FS coupling to a $U(1)$ gauge field. In contrast to Yukawa vertex $\psi^\dagger \psi \phi$, our vertex $\psi^\dagger \nabla \psi \mathbf{a}$ receives an extra factor $(\mathbf{k}_1 + \mathbf{k}_2)/2$. Consequently, the MT diagram (4.6) becomes

$$\int d\omega_1 d\omega_2 d\mathbf{k}_1 d\mathbf{k}_2 d\mathbf{q} \mathbf{k}_1 \mathbf{k}_2 (\mathbf{k}_1 + \mathbf{k}_2)_\mu (\mathbf{k}_1 + \mathbf{k}_2)_\nu G(i\omega_1, \mathbf{k}_1) G(i(\omega_1 + \Omega_m), \mathbf{k}_1) \times G(i\omega_2, \mathbf{k}_2) G(i(\omega_2 + \Omega_m), \mathbf{k}_2) \cdot D(i(\omega_1 - \omega_2), \mathbf{q}), \quad (4.7)$$

whose non-vanishing part is an even function of \mathbf{k}_i . In other words, the MT diagram is not zero in our model. As is shown in section 2 and 3, the MT diagram precisely cancels the self-energy contribution to the polarisation. To obtain linear- T resistivity, we have to consider the two-loop diagram (2.17). Though sharing the similar qualitative behaviour, The linearity of random Yukawa model is from $\mathbf{A} \psi^\dagger \nabla \psi$, whereas

Decay-rate argument The strange metal analysis above is from the view of the quantum field theory. Alternatively, one can also apply eqn.(4.1) to find the dependence on temperature. As is shown in Fig.2 below, three particles are involved in this process. A boson with wave-vector \mathbf{q} scatters an electron with momentum \mathbf{k}_1 to the one with \mathbf{k}_2 , and the scattering angle θ is very small at low temperature. In this case, the source of resistivity is boson, so the DoS is evaluated over boson wavevector \mathbf{q} unlike the 4-fermion interaction model of Fermi liquid.

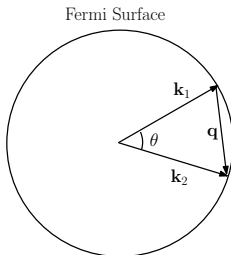


Figure 2. An illustration of an electron-boson scattering at low temperatures.

Consider a theory in d -spatial dimension with a bosons whose dispersion relation is $\epsilon \sim \mathbf{q}^\alpha$. Then the decay rate contribution from DoS of these bosons are

$$\int d^d \mathbf{q} \frac{1}{e^{\beta\epsilon} - 1} \sim T^{d/\alpha} \int dx \frac{x^{(d-\alpha)/\alpha}}{e^x - 1}. \quad (4.8)$$

In the last step, we set $\beta\epsilon = x$ and we used the fact that for low temperature case ($\beta \sim \infty$) the integration limit of x is approximately from 0 to ∞ . Therefore, the scattering rate contains a factor of $T^{d/\alpha}$ from DoS. On the other hand, the angular dependence here contributes to the temperature power unless the model has a spatially random coupling, because

$$(1 - \cos \theta) \simeq \frac{\mathbf{q}^2}{k_F^2} \sim \epsilon^{2/\alpha} / k_F^2 \sim T^{2/\alpha} x^{2/\alpha} / k_F^2. \quad (4.9)$$

Then from eqn.(4.1),(4.8) and (4.9), the resistivity is $T^{(d+2)/\alpha}$.

In spatially uniform model [17–19], our model, and spatially random Yukawa theory [17], the bosonic self-energies are all approximately linear in frequency, taking similar form with eqn. (2.22). The bosonic propagator then reads

$$D(i\Omega_m, \mathbf{q}) \simeq \frac{1}{\mathbf{q}^2 + c_0 |\Omega_m|}, \quad (4.10)$$

so poles are along $\epsilon \sim \mathbf{q}^2$. Therefore, $\alpha = 2$ and the contribution from DoS of bosons is $T^{d/2}$ according to (4.8). For the $(1 - \cos \theta)$ contribution, two cases are different.

1. For the model with uniform coupling for both with and without randomness, $(1 - \cos \theta) \sim \theta^2 \sim \mathbf{q}^2 \sim \epsilon \sim T$. Taking $d = 2$, the total transport scattering rate is proportional to T^2 , which matches the result in [18]. Unlike the resistivity of Fermi liquids which is T^2 in all dimensions, the quadratic resistivity from (random) Yukawa coupling with random potential only appears in $(2 + 1)$ dimensions.

2. On the other hand, for the models with space dependent random couplings, the presence of delta function in the correlator of couplings removes the contribution from $(1 - \cos \theta)$ ³. In such models, bosons can always relax the electric current even for very low temperatures. Consequently, the resistivity gets the power of T only from the contribution of DoS only, which is linear in T . Therefore in this model the unusually fast relaxation of strange metal is originated from the correlation of space dependent random couplings. Whether such random correlation can be attributed to the strong coupling nature of the material is not clear.

A summary of three models discussed in this section is given as Table 1. Since all these models includes impurities, the table only shows the dependence on temperature from various interaction types.

scattering type	DoS	$1 - \cos \theta$	resistivity
$u\psi^\dagger\psi^\dagger\psi\psi$	T^2	T^0	T^2
$g_{ijk}\phi_i\psi_j^\dagger\psi_k$	T	T	T^2
$g_{ijk}(\mathbf{r})\phi_i\psi_j^\dagger\psi_k$	T	T^0	T

Table 1. Temperature dependence from DoS and $1 - \cos \theta$ for each models. We assumed $d = 2$ for the Yukawa models, and in all cases we did not mention the residual resistivity ρ_0 from impurities.

Based on the discussion above, eqn.(4.1) gives

$$\rho \sim \begin{cases} T^{(d+2)/\alpha}, & \text{without the spatial dependence of the random coupling} \\ T^{d/\alpha}, & \text{with the spatial dependence of the random coupling} \end{cases} \quad (4.11)$$

for electron-boson scatterings. So far all the strange metal comes from the case with $d = 2 = \alpha$ with spatial disorder. One may get linear resistivity for a theory without spatial disorder if $\alpha = d + 2$. Such theory is plausible only if one can get the boson self energy $\Pi \sim \Omega/\rho^d$. Construction of such theory is not a trivial task and is left for a future work.

The $\hat{\mathbf{R}}\hat{\mathbf{o}}\hat{\mathbf{l}}\hat{\mathbf{e}}$ of potential disorder The previous subsection shows that the spatial randomness in Yukawa type couplings alters a quadratic resistivity to a linear one. Here we briefly discuss the $\hat{\mathbf{r}}\hat{\mathbf{o}}\hat{\mathbf{l}}$ e of potential disorder $v_{ij}(\mathbf{r})\psi_i^\dagger\psi_j$. A more detailed summary over various models is presented in Appendix A

Typically, the potential disorder brings impurities to a model, resulting in a constant residue resistivity ρ_0 [17, 18, 45]. Its $\hat{\mathbf{r}}\hat{\mathbf{o}}\hat{\mathbf{l}}$ e, however, is more than contributing a constant resistivity. In [27], the authors find that for spatially uniform clean model characterised by $g\psi^\dagger\psi\phi$ (or $g_{ijl}\psi_i^\dagger\psi_j\phi_l$ in [19]), where an FS coupled to a $U(1)$ gauge field without potential disorder, there would be a resistivity $\rho \sim T^{4/3}$ from electron-boson scattering. It was shown in [18] that such resistivity is *zero* as consequence of cancellation by the diagrams not considered in [27].

³The contribution from $(1 - \cos \theta)$ is obtained only when momentum conservation is imposed.

For spatially random Yukawa model $g_{ijl}(\mathbf{r})\psi_i^\dagger\psi_j\phi_l$, the qualitative behaviour is almost the same after one turns off the potential disorder. Without $v_{ij}(\mathbf{r})\psi_i^\dagger\psi_j$, the electron-boson scattering still yields a linear- T resistivity [19], except that there will be no residue resistivity ρ_0 .

5 Conclusion and Outlooks

In this paper, an FS coupled to a $U(1)$ gauge field is studied, where the couplings are characterised by spatial random disorder. One achievement of this paper, as we have seen in section 2 and section 3, is that we verify the rôle of spatial random coupling between electrons and bosons is independent of the boson types. In two-dimensional space, it leads to strange-metal behaviour at low temperatures. When it is generalised to $(3+1)$ D, the resistivity is no longer linear in temperatures. This indicates that at least in $(2+1)$ -dimensional systems, the spatial random fermion-boson couplings can be a master key for linear- T resistivity.

Based on the computation, we tried to find an intuitive way to interpret the linearity caused by spatial random coupling. It has two effects, which work together to bring a system a linear resistivity. The delta function over the coordinate space relaxes the momentum conservation of a scattering process, and this removes the small-angle corrections. Consequently, the scattering rate will be only proportional to the number of bosons. Since the boson propagator peaks at $\Omega_{\mathbf{q}} \sim \mathbf{q}^2$, the DoS $\sim T$, i.e. the resistivity is linear in T . Moreover, we find two possible way to reach linear T resistivity: one by $\Omega_{\mathbf{q}} \sim \mathbf{q}^{d+2}$ without spatial random coupling and the other by $\Omega_{\mathbf{q}} \sim \mathbf{q}^d$ without spatial random coupling. It depends on whether the polarisation receives vertex corrections or not. It is of future interest to build various candidates of strange metal according to this criteria.

One may ask what is the origin of the gauge field appearing in this work. In fact, gauge field coupled with fermions has been widely investigated [26, 27, 35, 46–50]. Such a system is related with fractional quantum hall effects and high-temperature superconductivity [27]. The $U(1)$ gauge field can be either emergent one or it can also be simply an electromagnetic field. For our purpose, the origin of this gauge field is not important, since the emphasis is to check the universality of the method suggested in [17] and show that it is independent of the interaction type.

The most tantalizing question left is whether the realization of the random spatial disorder has any connection to the strongly coupled system in its origin. While all the calculation in this work as well as in [30] were performed with the assumption of weak coupling, the actual material showing the strange metallicity are all strongly correlated ones. Without such connection, the mechanism would be still remote to the nature.

There are still lots of aspects to be studied before a rigorous theory of strange metal is constructed. It is also interesting to investigate the scaling of critical temperature of

superconductivity in this type of models. Recently, it was observed that at low temperatures, if a system has a resistivity $\rho = \rho_0 + AT$, then its critical temperature can satisfy $T_c \propto A^{1/2}$ [51, 52]. As is shown in this paper and in [30], A is proportional to K^2 (or g^2) which is coupling constant between fermions and bosons. This provides a testing ground for the theory described by eqn.(2.2). It has been found in spatially random Yukawa model, $T_c \sim A$ instead of $A^{1/2}$ [53]. If one can find that in vector models, $T_c \sim K$, then reliability of our model can be further improved.

Another aspect to be explored is to flesh out the model (2.8) with more physical details. For example, the presence of external magnetic field can be investigated. Here we only study the conductivity of the system, but in addition to the linear- T resistivity, a Hall angle $\sim T^2$ is another important feature of cuprate strange metal [54, 55]. Therefore, the behaviour of Hall angle provides a criteria to verify if the model (2.8) describe certain types of strange metal.

Finally, holography has turned out to be a powerful tool studying the condensed matter system [56–58]. For instance, the linear- T conductivity as well as the quadratic- T Hall angle can be realised by a black hole [59, 60]. In [61], the authors use holographic formalism to study the quantum critical points. Therefore, developing the holographic description and exploring phenomenology can be an interesting topic in the future.

Acknowledgments

The authors would like to thank Yunkyung Bang, Yu-Ge Chen, Han-Yong Choi, Yi Zhang, and Difan Zhou for the insightful discussion. This work is partly supported by NSFC, China (Grant No. 12275166 and No. 12311540141). This work is also supported by NRF of Korea with grant No. NRF-2021R1A2B5B02002603, RS-2023-00218998 and NRF-2022H1D3A3A01077468.

A A brief Summary of a few Models

This appendix is a complement of section 4, and we will present a brief review on several relevant models and generalise Bloch’s argument to these models as well.

This paper following the line of [17] shows that spatially random interactions offer one approach to the theory of strange metal. In section 4, we interpret the linear resistivity by simply counting DoS and small-angle correction via eqn.(4.1). Now let us delve into the underlying mechanism, illustrating the effects of the random spatial disorder with more detail. To this end, we first summarize the contents of [17–19]. Since the FS coupled to scalar and FS coupled to vector share the same qualitative properties, we take models based on the scalar type Yukawa coupling for simplicity.

Now we consider the effects of potential disorder $v(\mathbf{r})\psi^\dagger(\mathbf{r})\psi(\mathbf{r})$ without flavour indices [25]. Usually one takes $\langle v(\mathbf{r}) \rangle = 0$ and $\langle v^*(\mathbf{r})v(\mathbf{r}') \rangle = v^2 f(\mathbf{r} - \mathbf{r}')$. Its first-order contribution to the resistivity is $\mathcal{O}(T^0)$ ⁴. Generally, there exists vertex corrections [29], and the total resistivity can be evaluated from the following Feynman diagram,


(A.1)

which contains an angular average. If we take $f(\mathbf{r} - \mathbf{r}') \sim \delta(\mathbf{r} - \mathbf{r}')$, there is no vertex correction [17], hence the total polarization has a simple form given in (2.28). In addition, a potential $v_{ij}\psi_i^\dagger(\mathbf{r})\psi_j(\mathbf{r})$, which is disordered only in flavour space without spatial dependence with zero mean, brings no contribution, because it leaves the Fermionic propagator unchanged.

Let us continue to the interaction between the fermions and the $U(1)$ gauge field in $(2+1)$ dimension. The computation in [27], where the Fermi surface coupled with a $U(1)$ gauge field without disorder was studied, provides us guide to study this type of models [18]. According [27], a part of MT diagram (2.31) cancels the self-energy contribution, and the rest part of MT diagram, together with AL diagrams (2.32) should yield a resistivity $\rho \sim T^{4/3}$.

The scaling behaviour is further verified in [18], where a random Yukawa term $g_{ijk}\phi_i\psi_j^\dagger\psi_k$ is studied *without* potential disorder, so it also named a clean random Yukawa model. In this theory, the random disorder is introduced. However, the colour disorder does not change the fundamental properties of the model, and the authors also find the contribution from MT and AL diagrams would result in a resistivity $\rho \sim T^{4/3}$.

So it seems that the total contributions result in a conductivity $\sigma^{xx} \sim T^{-2/3}$, or a resistivity $\rho \sim T^{4/3}$ [27]. However, the calculation in [27] is corrected by [18] such that the summation of all diagrams is zero. In other words, the coefficient of $T^{4/3}$ is 0. The absence of resistivity from electron-boson scattering is a result of “boson drag” [16–18], as will be illustrated later. One main conclusion here is that the random coupling alone cannot lead to a theory of strange metal.

As mentioned in section 4, after introducing a spatial disorder potential $v_{ij}(\mathbf{r})\psi_i^\dagger\psi_j$, it was shown in [17, 18] that the electron self-energy reads $\omega \ln(1/\omega)$. The presence of impurity widens the peak at the Fermi surface [18], and this brings a overwhelmingly large scattering rate Γ which is of order ω^0 . Therefore, in the computation of Dyson’s equations we can drop many higher-order terms in ω . The computation shows that the Feynman

⁴The introduction of flavour in the disorder potential $v(\mathbf{r}) \rightarrow v_{ij}(\mathbf{r})$ hardly changes the property, so we will not think of $v_{ij}(\mathbf{r})\psi_i^\dagger(\mathbf{r})\psi_j(\mathbf{r})$ separately.

graph

$$(A.2)$$

contributes the conductivity a term linear in temperature. However, such linear- T dependence is precisely canceled by the MT diagrams (2.31) [17, 18]. Due to this cancellation, the higher order AL diagrams finally brings a resistivity $\rho \sim T^2$ [18]. As a consequence, there is no strange-metal behaviour either in this theory [17, 18]. Despite the failure, the theory achieved the realization that the spatial random disorder is very likely the steppingstone to the strange metal.

Finally, the authors of [17] find a way to get rid of the cancellation of MT graphs. The key is the spatial dependence of the coupling $g_{ijk}(\mathbf{r})$ in the interaction term $g_{ijk}(\mathbf{r})\phi_i\psi_j^\dagger\psi_k$, which satisfies

$$\langle g_{ijk}^*(\mathbf{r})g_{i'j'k'}(\mathbf{r}') \rangle = g^2\delta(\mathbf{r} - \mathbf{r}')\delta_{ii'}\delta_{jj'}\delta_{kk'}.$$

Because of the spatial delta, the MT diagram and AL diagrams vanish, and the only contribution is from eqn.(A.2) so that the terms linear- T survives. Additionally, in [19], the authors find that the spatially random Yukawa coupling can yield a linear- T resistivity even without the potential disorder.

In short, the flavour disordered Yukawa(-like) couplings hardly change the physical properties, but the *spatial disorder* is the key to obtain strange-metal behaviour, as is summarised in table where we have compared various typical electron-boson scattering models. 2.

scattering type	resistivity
$v_{ij}(\mathbf{r})\psi_i^\dagger\psi_j$	$\sim \rho_0$
$v_{ij}\psi_i^\dagger\psi_j$	no contribution
$u\psi^\dagger\psi^\dagger\psi\psi + \text{impurities}$	$\sim \rho_0 + AT^2$
$g\phi\psi^\dagger\psi$	$\mathcal{T}^{4/3}$ absence
$g_{ijk}\phi_i\psi_j^\dagger\psi_k$	$\mathcal{T}^{4/3}$ absence
$g_{ijk}\phi_i\psi_j^\dagger\psi_k + v_{ij}(\mathbf{r})\psi_i^\dagger\psi_j$	$\sim \rho_0 + AT + BT^2$
$g_{ijk}(\mathbf{r})\phi_i\psi_j^\dagger\psi_k$	$\sim T$
$g_{ijk}(\mathbf{r})\phi_i\psi_j^\dagger\psi_k + v_{ij}(\mathbf{r})\psi_i^\dagger\psi_j$	$\sim \rho_0 + AT$

Table 2. A comparison among models with and without spatial random couplings.

Now let us continue to the mechanism for the linear- T resistivity. One may wonder why the linear- T resistivity is so hard to get and why it is obtained only in spatial dimensions 2. This subsection will offer some intuitive discussion following section 4. The

electron-boson scattering described by Fig.2 yields a resistivity. The resistivity consists of contributions from DoS of bosons, $T^{d/\alpha}$, and small-angle contributions, $T^{2/\alpha}$.

Now let us test the models mentioned above. The relation $\epsilon_{\mathbf{q}}$ can be derived from bosonic propagator $\Pi(i\Omega, \mathbf{q})$. In both regular Yukawa model [27] and the clean random Yukawa [19], the boson self-energy is given by [18]

$$\Pi(i\Omega_m, \mathbf{q}) = -c_g \frac{|\Omega_m|}{|\mathbf{q}|}, \quad (\text{A.3})$$

where c_g is a constant. So the bosonic propagator is

$$D(i\Omega_m, \mathbf{q}) \simeq \frac{1}{\mathbf{q}^2 + c_g \frac{|\Omega_m|}{|\mathbf{q}|}}. \quad (\text{A.4})$$

This implies that the pole of the boson propagator comes from

$$\Omega_m \sim \mathbf{q}^3, \quad (\text{A.5})$$

i.e. $\alpha = 3$. According to (4.8), it gives DoS contribution to the scattering rate $T^{d/3}$. Similarly, the small-angle scattering gives $T^{2/3}$. As a result, the total transport scattering rate depends on $T^{(d+2)/3}$. Taking $d = 2$, one recovers the resistivity in a Yukawa-like theory where $\rho \sim T^{4/3}$ [27]. However, as is shown in [18], this would-be $T^{4/3}$ -dependence turns out to contribution from other diagrams.

In systems without impurities, there exists ‘*boson drag*’ resulting in an absent resistivity [16–18]. Though following Bloch’s argument, one should find the resistivity satisfies $\rho \sim T^{4/3}$, Peierls argues that “phonon drag” will make the resistivity decreases faster than one expects from eqn.(4.1) [43, 62, 63]. When temperatures is low enough such that the umklapp process cannot happen, the *total* momentum of bosons and fermions is conserved in a clean model. The decay of electric current becomes infinitely slow, so, as is shown in [18], the scattering is unable contribute and the resistivity vanishes. Therefore, in models with global momentum conservation, eqn.(4.1) is not appropriate for achieving the resistivity, and we should expect a vanishing resistivity due to “boson drag” [16]. The conservation of total momentum is necessary for boson drag to happen, so for the time being, phonon drag is only observed in very pure sample [16, 17, 64]. In the presence of impurities, the total momentum will decline and there will no boson drag.

Now let us see how the result is changed by introducing potential disorder $v(\mathbf{r})\psi^\dagger\psi$ [18]. Such impurity potential not only prevents the system from boson drag by breaking the global momentum conservation, but also alters the behavior of the boson propagator. Because the self energy Π becomes $\Omega/\sqrt{\Gamma^2 + q^2}$ and $\Gamma \gg q$ so that the bosonic propagator reads

$$D(i\Omega_m, \mathbf{q}) \simeq \frac{1}{\mathbf{q}^2 + c_0|\Omega_m|}. \quad (\text{A.6})$$

Then poles are along $\epsilon \sim \mathbf{q}^2$ so that dispersion relation changes drastically. With $\alpha = 2$, one finds $\rho \sim T^{(d+2)/2}$ according to eqn.(4.1). Choosing $d = 2$, one finds the result in [18] with a resistivity $\sim T^2$ due to the vertex corrections from AL digrams.

As summarised in section 4, there is no correction from $(1 - \cos \theta)$ in spatially random Yukawa model. Only DoS begets a $T^{d/2}$ resistivity. Moreover, the spatial randomness dropped the momentum conservation on vertices and the global momentum conservation is broken as well. Therefore even without impurities, boson drag is impossible to happen in a clean spatially random system [19]. Hence when $d = 2$, the spatially random Yukawa coupling yields a resistivity linear in T . While in $(3 + 1)$ dimensions, this property disappears and one finds $\rho \sim T^{3/2}$. This result of $(3 + 1)$ dimensions is not only consistent with [17], but also section 3 in this article. Furthermore, based on this analysis, one finds that the result is qualitatively the same regardless of which type of bosons (scalar or vector) the electrons are coupled to, since only the relation $\epsilon(\mathbf{q})$ and spatial dimensions contribute.

In essence, eqn.(4.11) can be further modified into table 3. Suppose we have a system of $(d + 1)$ dimensions where FS coupled to critical bosons. In order that the scattering has non-trivial contribution to the resistivity, the first step is to break the total momentum conservation of bosons and electrons. This can be achieved by either introducing impurities (such as potential disorder) or spatial disorder. Then the resistivity $\rho \sim T^{(d+2/\alpha)}$ for spatially uniform couplings, and $\rho \sim T^{d/\alpha}$ for spatially random couplings.

spatial disorder	global momentum conservation	resistivity
×	√	absent
×	×	$T^{(d+2)/\alpha}$
√	×	$T^{d/\alpha}$

Table 3. The resistivity from electron-boson scatterings.

References

- [1] P.A. Lee, N. Nagaosa and X.-G. Wen, *Doping a mott insulator: Physics of high-temperature superconductivity*, *Rev. Mod. Phys.* **78** (2006) 17.
- [2] P.W. Anderson, *The theory of superconductivity in the high- T_c cuprates*, Princeton University Press (2017).
- [3] S.-S. Lee, *Recent Developments in Non-Fermi Liquid Theory*, *Ann. Rev. Condensed Matter Phys.* **9** (2018) 227 [1703.08172].
- [4] R.L. Greene, P.R. Mandal, N.R. Poniatowski and T. Sarkar, *The strange metal state of the electron-doped cuprates*, *Annual Review of Condensed Matter Physics* **11** (2020) 213 [<https://doi.org/10.1146/annurev-conmatphys-031119-050558>].
- [5] C.M. Varma, *Colloquium: Linear in temperature resistivity and associated mysteries including high temperature superconductivity*, *Rev. Mod. Phys.* **92** (2020) 031001.

- [6] S.A. Hartnoll and A.P. Mackenzie, *Colloquium: Planckian dissipation in metals*, *Rev. Mod. Phys.* **94** (2022) 041002 [2107.07802].
- [7] P.W. Phillips, N.E. Hussey and P. Abbamonte, *Stranger than metals*, *Science* **377** (2022) abh4273 [2205.12979].
- [8] M. Gurvitch and A.T. Fiory, *Resistivity of $\text{La}_{1.825}\text{Sr}_{0.175}\text{CuO}_4$ and $\text{YBa}_2\text{Cu}_3\text{O}_7$ to 1100 K: Absence of saturation and its implications*, *Phys. Rev. Lett.* **59** (1987) 1337.
- [9] H. Takagi, B. Batlogg, H.L. Kao, J. Kwo, R.J. Cava, J.J. Krajewski et al., *Systematic evolution of temperature-dependent resistivity in $\text{La}_{2-x}\text{Sr}_x\text{CuO}_4$* , *Phys. Rev. Lett.* **69** (1992) 2975.
- [10] H.v. Lohneysen, A. Rosch, M. Vojta and P. Wolfe, *Fermi-liquid instabilities at magnetic quantum phase transitions*, *Rev. Mod. Phys.* **79** (2007) 1015 [cond-mat/0606317].
- [11] P. Monthoux, D. Pines and G. Lonzarich, *Superconductivity without phonons*, *Nature* **450** (2007) 1177–1183.
- [12] T. Shibauchi, A. Carrington and Y. Matsuda, *A quantum critical point lying beneath the superconducting dome in iron pnictides*, *Annual Review of Condensed Matter Physics* **5** (2014) 113.
- [13] B. Michon, C. Girod, S. Badoux, J. Kačmarčík, Q. Ma, M. Dragomir et al., *Thermodynamic signatures of quantum criticality in cuprate superconductors*, *Nature* **567** (2019) 218–222.
- [14] S. Sachdev and J. Ye, *Gapless spin-fluid ground state in a random quantum heisenberg magnet*, *Phys. Rev. Lett.* **70** (1993) 3339.
- [15] A. Kitaev, *A simple model of quantum holography*, *Talk at KITP Program: Entanglement in Strongly-Correlated Quantum Matter* (2015) .
- [16] D. Chowdhury, A. Georges, O. Parcollet and S. Sachdev, *Sachdev-Ye-Kitaev models and beyond: Window into non-Fermi liquids*, *Rev. Mod. Phys.* **94** (2022) 035004 [2109.05037].
- [17] A.A. Patel, H. Guo, I. Esterlis and S. Sachdev, *Universal theory of strange metals from spatially random interactions*, *Science* **381** (2023) abq6011 [2203.04990].
- [18] H. Guo, A.A. Patel, I. Esterlis and S. Sachdev, *Large- N theory of critical Fermi surfaces. II. Conductivity*, *Phys. Rev. B* **106** (2022) 115151 [2207.08841].
- [19] I. Esterlis, H. Guo, A.A. Patel and S. Sachdev, *Large N theory of critical Fermi surfaces*, *Phys. Rev. B* **103** (2021) 235129 [2103.08615].
- [20] A. Georges, O. Parcollet and S. Sachdev, *Quantum fluctuations of a nearly critical heisenberg spin glass*, *Phys. Rev. B* **63** (2001) 134406.
- [21] S. Sachdev, *Bekenstein-Hawking Entropy and Strange Metals*, *Phys. Rev. X* **5** (2015) 041025 [1506.05111].
- [22] J. Maldacena and D. Stanford, *Remarks on the Sachdev-Ye-Kitaev model*, *Phys. Rev. D* **94** (2016) 106002 [1604.07818].
- [23] A. Kitaev and S.J. Suh, *The soft mode in the Sachdev-Ye-Kitaev model and its gravity dual*, *JHEP* **05** (2018) 183 [1711.08467].
- [24] S. Sachdev, *Strange metals and black holes: Insights from the sachdev-ye-kitaev model*, 12, 2023. 10.1093/acrefore/9780190871994.013.48.

- [25] A. Altland and B. Simons, *Condensed matter field theory*, Cambridge University Press (2023).
- [26] B.I. Halperin, P.A. Lee and N. Read, *Theory of the half-filled Landau level*, *Phys. Rev. B* **47** (1993) 7312.
- [27] Y.B. Kim, A. Furusaki, X.-G. Wen and P.A. Lee, *Gauge-invariant response functions of fermions coupled to a gauge field*, *Phys. Rev. B* **50** (1994) 17917 [[cond-mat/9405083](#)].
- [28] S.-S. Lee, *Low energy effective theory of Fermi surface coupled with $U(1)$ gauge field in 2+1 dimensions*, *Phys. Rev. B* **80** (2009) 165102 [[0905.4532](#)].
- [29] P. Coleman, *Introduction to many-body physics*, Cambridge University Press (2019).
- [30] A.A. Patel, P. Lunts and S. Sachdev, *Localization of overdamped bosonic modes and transport in strange metals*, [2312.06751](#).
- [31] L.H. Ryder, *Quantum Field theory*, Cambridge University Press (1996).
- [32] G.D. Mahan, *Many-particle physics*, Springer (2014).
- [33] L.B. Ioffe and G. Kotliar, *Transport phenomena near the Mott transition*, *Phys. Rev. B* **42** (1990) 10348.
- [34] G. Baskaran and P.W. Anderson, *Gauge theory of high-temperature superconductors and strongly correlated Fermi systems*, *Phys. Rev. B* **37** (1988) 580.
- [35] L.B. Ioffe and P.B. Wiegmann, *Linear temperature dependence of resistivity as evidence of gauge interaction*, *Phys. Rev. Lett.* **65** (1990) 653.
- [36] P.B. Wiegmann, *Superconductivity in strongly correlated electronic systems and confinement versus deconfinement phenomenon*, *Phys. Rev. Lett.* **60** (1988) 821.
- [37] P. Wiegmann, *Towards a gauge theory of strongly correlated electronic systems*, *Physica C: Superconductivity* **153-155** (1988) 103.
- [38] Y. Gu, A. Kitaev, S. Sachdev and G. Tarnopolsky, *Notes on the complex Sachdev-Ye-Kitaev model*, *JHEP* **02** (2020) 157 [[1910.14099](#)].
- [39] D.H. Nguyen, A. Sidorenko, M. Taupin, G. Knebel, G. Lapertot, E. Schuberth et al., *Superconductivity in an extreme strange metal*, *Nature Communications* **12** (2021) .
- [40] A. Legros, S. Benhabib, W. Tabis, F. Laliberté, M. Dion, M. Lizaire et al., *Universal t -linear resistivity and Planckian dissipation in overdoped cuprates*, *Nature Physics* **15** (2018) 142–147.
- [41] F. Bloch, *Über die Quantenmechanik der Elektronen in Kristallgittern*, *Zeitschrift für Physik* **52** (1929) 555.
- [42] F. Bloch, *Zum elektrischen Widerstandsgesetz bei tiefen Temperaturen*, *Zeitschrift für Physik* **59** (1930) 208.
- [43] N.W. Ashcroft and N.D. Mermin, *Solid state physics*, Cengage (1976).
- [44] S. Sachdev, *Quantum Phase Transitions*, Cambridge University Press (2011).
- [45] S. Hartnoll, A. Lucas and S. Sachdev, *Holographic quantum matter*, The MIT Press (2018).
- [46] J. Polchinski, *Low-energy dynamics of the spinon gauge system*, *Nucl. Phys. B* **422** (1994) 617 [[cond-mat/9303037](#)].

- [47] B.L. Altshuler, L.B. Ioffe and A.J. Millis, *Low-energy properties of fermions with singular interactions*, *Phys. Rev. B* **50** (1994) 14048.
- [48] P.A. Lee, *Low-temperature t -linear resistivity due to umklapp scattering from a critical mode*, *Phys. Rev. B* **104** (2021) 035140.
- [49] F. Schlawin, A. Cavalleri and D. Jaksch, *Cavity-mediated electron-photon superconductivity*, *Phys. Rev. Lett.* **122** (2019) 133602.
- [50] P. Rao and F. Piazza, *Non-fermi-liquid behavior from cavity electromagnetic vacuum fluctuations at the superradiant transition*, *Phys. Rev. Lett.* **130** (2023) 083603.
- [51] J. Yuan, Q. Chen, K. Jiang, Z. Feng, Z. Lin, H. Yu et al., *Scaling of the strange-metal scattering in unconventional superconductors*, *Nature* **602** (2022) 431–436.
- [52] X. Jiang, M. Qin, X. Wei, L. Xu, J. Ke, H. Zhu et al., *Interplay between superconductivity and the strange-metal state in fese*, *Nature Physics* **19** (2023) 365.
- [53] C. Li, D. Valentinis, A.A. Patel, H. Guo, J. Schmalian, S. Sachdev et al., *Strange metal and superconductor in the two-dimensional Yukawa-Sachdev-Ye-Kitaev model*, **2406.07608**.
- [54] M. Blake and A. Donos, *Quantum Critical Transport and the Hall Angle*, *Phys. Rev. Lett.* **114** (2015) 021601 [[1406.1659](#)].
- [55] J.R. Schrieffer and J. Brooks, *Handbook of high-temperature superconductivity: Theory and experiment*, Springer (2014).
- [56] C.P. Herzog, *Lectures on Holographic Superfluidity and Superconductivity*, *J. Phys. A* **42** (2009) 343001 [[0904.1975](#)].
- [57] S.A. Hartnoll, *Lectures on holographic methods for condensed matter physics*, *Class. Quant. Grav.* **26** (2009) 224002 [[0903.3246](#)].
- [58] J. McGreevy, *Holographic duality with a view toward many-body physics*, *Adv. High Energy Phys.* **2010** (2010) 723105 [[0909.0518](#)].
- [59] X.-H. Ge, Y. Tian, S.-Y. Wu and S.-F. Wu, *Hyperscaling violating black hole solutions and Magneto-thermoelectric DC conductivities in holography*, *Phys. Rev. D* **96** (2017) 046015 [[1606.05959](#)].
- [60] X.-H. Ge, Y. Tian, S.-Y. Wu and S.-F. Wu, *Linear and quadratic in temperature resistivity from holography*, *JHEP* **11** (2016) 128 [[1606.07905](#)].
- [61] X. Huang, S. Sachdev and A. Lucas, *Disordered Quantum Critical Fixed Points from Holography*, *Phys. Rev. Lett.* **131** (2023) 141601 [[2306.03130](#)].
- [62] R. Peierls, *Zur Theorie der elektrischen und thermischen Leitfähigkeit von Metallen*, *Annalen der Physik* **396** (1930) 121 [<https://onlinelibrary.wiley.com/doi/pdf/10.1002/andp.19303960202>].
- [63] R. Peierls, *Zur Frage des elektrischen Widerstandsgesetzes für tiefe Temperaturen*, *Annalen der Physik* **404** (1932) 154 [<https://onlinelibrary.wiley.com/doi/pdf/10.1002/andp.19324040203>].
- [64] C.W. Hicks, A.S. Gibbs, A.P. Mackenzie, H. Takatsu, Y. Maeno and E.A. Yelland, *Quantum oscillations and high carrier mobility in the delafossite pdcoo_2* , *Phys. Rev. Lett.* **109** (2012) 116401.